
ENDOGENOUS MODULATION OF DELTA PHASE BY EXPECTATION

—

A REPLICATION OF STEFANICS ET AL., 2010

Sophie K Herbst*

Cognitive Neuroimaging Unit, NeuroSpin, INSERM, CEA, CNRS, Université Paris-Saclay
Bât 145, Gif s/ Yvette 91190, France

Gabor Stefanics

Translational Neuromodeling Unit (TNU), Institute for Biomedical Engineering,
University of Zurich & ETH Zurich, Switzerland

Jonas Obleser

Department of Psychology, University of Lübeck
Ratzeburger Allee 160, 23552 Lübeck, Germany

Center of Brain, Behavior, and Metabolism, University of Lübeck
Ratzeburger Allee 160, 23552 Lübeck, Germany

January 31, 2022

ABSTRACT

The human brain efficiently extracts the temporal statistics of sensory environments and automatically generates expectations about future events. An influential hypothesis holds that these expectations can find their implementation in neural oscillations, notably in the delta band (0.5–3 Hz). Rhythmic fluctuations of cortical excitement are thought to align and match up in phase to the temporal structure of the sensory environment. This alignment is thought to result in the more excitable phase range of neural oscillations to overlap with the predicted onset of sensory events which in turn results in more efficient processing of sensory input, especially so in audition. An unresolved issue concerns whether such phase-aligned rhythmic brain activity is driven exclusively by the exogenous temporal structure of the input, or it also reflects phase re-alignment due to endogenous expectations based on stimulus probability and task relevance. In a seminal study, Stefanics et al. (2010) presented stimuli in a rhythmic stream and observed that delta phase consistency across trials was modulated by endogenous target onset expectations: delta phase consistency was higher prior to more probable (strongly expected) compared to less probable (weakly expected) target onsets. The present study replicates Experiment II of the original study, most importantly the modulation of delta phase consistency by endogenous expectations, and underlines a direct relationship between phase locking and behaviour. Our additional analyses locate the sources of the delta phase-alignment to motor, pre-motor, parietal, and temporal areas, and provide evidence for an ongoing delta oscillation, in line with the interpretation of oscillatory phase alignment rather than a transient evoked response. Importantly, this work shows that the phase of delta oscillations can be modulated by top-down control, and hence qualifies as a potential mechanism for the neural implementation of (rhythmic) temporal predictions.

*ksherbst@gmail.com

Keywords expectation · reaction time · task relevance · delta oscillations · EEG · phase consistency

Acknowledgements: The authors would like to thank Anne Herrmann, Franziska Scharata, and Martin Orf for help with setting up the experimental protocol and conducting pilot data recordings, Malte Naujokat, Jaro Janaschek, and Alexine Leroy for performing the data acquisition. This research was supported by a DFG grant (HE 7520/1-1) to SKH.

1 Introduction

2 Natural sensory environments commonly feature rhythmic or quasi-periodic temporal structures. In particular, auditory
3 inputs are constrained by rhythms at slow frequencies (Arnal and Giraud, 2012, Ding et al., 2017, Giraud and Poeppel,
4 2012, Jones and Boltz, 1989), which can facilitate the perceptual analysis of complex dynamic inputs. A large body of
5 research has shown that rhythmic input structures improve the detectability and processing speed of auditory stimuli
6 (Henry and Obleser, 2012, Herrmann et al., 2016, Lawrance et al., 2014, Rimmele et al., 2010, Stefanics et al., 2010,
7 Wright and Fitzgerald, 2004), as well as perceptual sensitivity (Chang et al., 2019, Jones et al., 2002, Morillon et al.,
8 2016, Schmidt-Kassow et al., 2009; but see Bauer et al., 2015).

9 Endogenously rhythmic brain dynamics prominently observed across species (Buzsáki and Draguhn, 2004), have been
10 hypothesized to provide an internal temporal structure on which external rhythms can be mapped (Herrmann and
11 Henry, 2014, Jones, 1976, Jones et al., 2002, Large and Jones, 1999). An influential proposal holds that slow neural
12 oscillations, notably in the delta frequency band (0.5–3 Hz), coordinate inter- and cross-modal attentional selection
13 in time by aligning in phase to an external rhythmic structure (Lakatos et al., 2008, Schroeder and Lakatos, 2009),
14 allowing to match states of high excitability with the expected onsets of future sensory events. Accordingly, a host
15 of studies using electrophysiological recordings of neural oscillations in humans have revealed evidence for phase
16 alignment to rhythmic inputs leading to modulation of behavior (Arnal et al., 2014, Besle et al., 2011, Cravo et al., 2013,
17 Henry et al., 2014, Henry and Obleser, 2012, Kösem et al., 2014, Morillon and Baillet, 2017, Stefanics et al., 2010,
18 van den Brink et al., 2014). In the literature, a number of terms exist to describe the phenomenon of synchronization
19 between internal and external rhythms (Lakatos et al., 2019, Obleser and Kayser, 2019), such as *phase locking*, *phase*
20 *consistency*, *entrainment*, and more. Here, we are interested in the *alignment* of the phase of neural oscillations to an
21 external rhythm, which surfaces as *phase consistency across trials*.

22 The overlap between external and internal rhythms raises the question to which extent the observed phase consistency
23 across trials reflects *entrainment* of an endogenous oscillation (Lakatos et al., 2019, Obleser and Kayser, 2019), versus
24 a mechanistically driven representation of the exogenous periodicity. An active role of entrainment in the attentional
25 selection process is suggested by its susceptibility to top-down influences such as the attended sensory modality (Keil
26 et al., 2016, Lakatos et al., 2008), task demands (Lakatos et al., 2013), perceptual grouping (Barczak et al., 2018), and
27 hierarchical rhythmic structure (Morillon and Baillet, 2017, Nozaradan et al., 2011). A seminal study by Stefanics
28 et al. (2010) showed that phase consistency of delta oscillations in the presence of an exogenous rhythm scales with the
29 strength of the expectation for a behaviorally relevant stimulus to occur in the next cycle of a rhythmic stimulus stream.
30 This result suggests that oscillatory phase alignment can be modulated endogenously to create a temporally transient
31 state of expectation.

32 A different set of studies have tested whether delta oscillations implement endogenous temporal predictions, indepen-
33 dently from periodic input structures. These studies used foreperiod paradigms (Niemi and Näätänen, 1981, Woodrow,
34 1914) in which temporal predictions are conveyed by single time intervals and need to be initiated on each trial (Breska
35 and Deouell, 2017, Cravo et al., 2011, Herbst and Obleser, 2017, 2018, Wilsch et al., 2015).

36 Only very few studies reported enhanced delta phase consistency in a non-rhythmic context (Breska and Deouell 2017,
37 Daume et al. 2021; but see Obleser et al. 2017) and for temporal predictions evoked by the passage of time (Wilsch et al.,
38 2015) using auditory stimuli, and one study reported enhanced phase consistency for temporally predicted visual stimuli
39 in theta band (4–7 Hz, Cravo et al., 2011). In three independent EEG experiments (total N = 70), using non-rhythmic
40 foreperiod manipulations, we did not observe phase consistency effects in the delta band *prior* to an expected target
41 onset (Herbst and Obleser, 2017, 2018). However, we have been able to show that listeners can flexibly form temporal
42 predictions associated to sensory features of temporal cues on a trial-by-trial basis (Herbst and Obleser, 2019), and
43 that these predictions enhance auditory sensitivity. Furthermore, using encoding-models, we could show that temporal
44 predictions are represented in human brain dynamics measured with EEG (Herbst et al., 2018). In Herbst and Obleser
45 (2019) we report a relationship between the phase of delta oscillations and auditory sensitivity in a temporally predictive
46 condition, which suggests a role of delta oscillations for non-rhythmic temporal predictions.

47 Thus, to date, it remains an open question to which extent the phase of cortical delta oscillations encodes *endogenous*
48 expectations derived from exogenous temporal structures. As the basis for an extended research program aiming at a
49 better understanding of the conditions under which delta oscillations could implement endogenous expectations, we
50 here set out to replicate the study described under Experiment II by Stefanics et al. (2010). This study consists in an
51 important basis for the research field outlined above, and at the time the current study was planned, the paper was cited
52 297 times. Human participants responded to pure tone stimuli, embedded in a rhythmic stream in which pitch cues
53 indicated whether a target occurred in the following first or second cycle with 20/ 80% versus 80/ 20% probability. The
54 authors reported a decrease in reaction times for targets occurring at the expected time points, and, crucially, relatively

55 enhanced phase consistency in the delta band (0.5–3 Hz) at time points for which strong (80%) versus weak (20%)
56 expectations existed.

57 Importantly, a hallmark feature of to-be replicated study, and an important part of our motivation to chose it for
58 replication, was its careful avoidance of confounding stimulus-evoked with pre-stimulus activity (Zoefel and Heil,
59 2013). By showing a modulation of stimulus-related rhythmic brain dynamics by expectation, the original study, and
60 now the replication, provide important evidence for an endogenous implementation of expectations in oscillatory brain
61 dynamics.

62 Here, we replicate the increase in delta phase consistency with expectation, which also correlated with the reaction
63 time benefits across individuals. In addition, we also examined whether the measured phase consistency qualifies as
64 an endogenous narrow-band oscillation that *entrains* to the stimulus rhythm, versus reflects more broad-band neural
65 activity. To achieve this, we performed additional spectral analyses on the data, and also assessed phase consistency
66 effects in the low delta (0.25–1.5 Hz) and theta (4–7 Hz) band.

67 To date, it is an open question to what extent the above-described oscillatory brain dynamics overlap with well-known
68 signatures of expectation observed in the time domain (both pre- and post- stimulus), such as the contingent negative
69 variation (Brunia, 2003, Mento, 2013, Walter et al., 1964), and the P300 (Ruchkin et al., 1980, Schröger et al., 2015,
70 Schürmann et al., 2001), for which the original study reported a partial overlap between with delta phase consistency.
71 In our view, it is possible that these different potentials result at least partially from a phase-reset of delta oscillatory
72 activity (Lakatos et al., 2008, Schürmann et al., 2001), and thus provide separate observation windows onto the same
73 neural activity.

74 Here, we addressed the overlap between oscillatory and time-domain measures, by performing a set of control analyses
75 in the spectral and temporal domain. Yet, a complete account of their respective nature will require a variety of study
76 designs (varying time windows, modalities, task requirements) and recording techniques (invasive recordings, enhanced
77 spatial resolution such as in MEG).

78 Hypotheses

79 In order to consider the replication successful, we assessed two main hypotheses:

80 **Hypothesis 1:** We expected to find a facilitatory effect of expectation on reaction times, that is, shorter reaction
81 times for targets that occur at the expected versus non-expected point in time. This effect was supposed to be
82 more pronounced at the short compared to the long time interval (**confirmed**).

83 **Hypothesis 2:** We expected to find that the strength of phase consistency in the delta band scales with the
84 expectation, such that stronger phase consistency would be observed when the expectation for a target to occur
85 was high (**confirmed**).

86 Additionally, we assessed several exploratory hypotheses:

87 **Hypothesis 3:** We expected to be able to isolate a peak in the EEG power spectrum that corresponds to the
88 stimulation frequency, separable from the 1/f scale-free activity (**confirmed**).

89 **Hypothesis 4a:** We expected the amplitude of target-evoked, broad-band responses to differ between expected
90 and unexpected targets, with no prior hypothesis on the direction for this difference (**post-target difference**
91 **not confirmed, but pre-target difference observed**).

92 **Hypothesis 4b:** We expected to see an omission response shortly after the time point of the early target
93 onset, but when no target occurred, with a larger amplitude on trials on which expectation was stronger (**not**
94 **confirmed**).

95 **Hypothesis 4c:** Correlation analyses were expected to show partial, but not full overlap between the time
96 domain signatures of expectation and delta phase consistency (**confirmed**).

97 **Hypothesis 5:** Following the confirmation of Hypothesis 2, we reconstructed the sources of the differences in
98 delta phase consistency, expecting them to lie mainly in auditory and possibly also motor areas (**confirmed**).

99 The preregistered Stage 1 report can be found under this link: <https://osf.io/w5eq4/>.

100 **Methods**

101 The auditory stimulation protocol was kept exactly as in the original study (Stefanics et al., 2010). A visual display,
102 which was not mentioned in the original study, was added to guide the participant throughout the task (see below).
103 Due to methodological advances in EEG research since the date of the original study, and the available facilities, our
104 (preregistered: <https://osf.io/w5eq4/>) analysis approach differed in some aspects from the to-be-replicated study.
105 All deviations from the original analysis approach are thought to reflect advances that should in all likelihood help to
106 uncover true effects and estimate their size more accurately.

107 **Participants**

108 **Ethical approval:** Ethical approval was obtained from the ethics committee of the University of Lübeck. All
109 participants signed informed consent and received either course credit or payment for their participation (10 € per
110 hour).

111 **Final participant sample:** The 26 participants considered for analysis had an average age of 23.61 years (SD: 3.56),
112 ten were male (ratio: 38.46%), and 21 were right-handed. Participants had no history of neurological or hearing disorder.
113 The original study tested 11 participants (6 female, no mention of handedness).

114 Using the stopping rule described below, we tested 28 participants, one of which was excluded due to an abortion of the
115 recording program, resulting in only 700 trials (see exclusion criteria below), and one due to too many trials rejected
116 during EEG preprocessing (566 trials left).

117 **Stopping rule:** Here, we applied an optional stopping approach using Bayes Factors (Rouder, 2014), to assess the
118 two main Hypotheses (the exact statistical tests are described in the Analyses section (pp. 6, 9):

119 **Hypothesis 1:** Reaction times are relatively shorter for strong versus weak expectations.

120 **Hypothesis 2:** Delta phase consistency is relatively higher for strong versus weak expectations.

121 Hypothesis 1 was confirmed, reaching a Bayes Factor of 3464.96. Concerning Hypothesis 2, we reached confirmatory
122 Bayes Factors of 7.40 (delta band), and 14.37 (low delta band). We initially stopped data recording at a Bayes Factor of
123 17 in favour of Hypothesis 2 (delta band), which turned out inflated due to a coding error and now lies at 7.40. Since the
124 results converge well across the different analyses, with the cluster-based permutation tests revealing robust levels of
125 significance, we decided to not take up testing again. The number of 26 participants included already exceeds that of
126 the original study (N=11).

127 **Recruitment criteria:** Initially, we invited 15 participants, and then continued until reaching conclusive Bayes
128 Factors for both Hypotheses 1 & 2: either > 10 in favour of the respective hypothesis, or < 0.1 in favour of the
129 corresponding H_0 . Due to practical constraints in recruiting and testing participants, we invited participants in groups
130 of five, and assessed the Bayes Factors after each group until we reached the target Bayes Factor. The final number
131 of 28 participants tested (not a multiple of five) resulted from cancellations by participants. Left- and right-handed
132 participants were recruited with a gender imbalance no larger than 60:40. Participants were required to have no
133 history of neurological or hearing disorder. If upon testing 50 participants we would not have reached a conclusion on
134 both hypotheses, we would have stopped the data collection, reported the results as inconclusive, and considered the
135 replication attempt as failed. Exclusion criteria are listed below.

136 **Recording abortion criteria:** Participants were granted the right to stop the experiment at any time without specifying
137 a reason. Furthermore, the experimenter could terminate the recording session in case of technical problems that either
138 made a recording impossible or would have lead to insufficient data quality.

139 **Post-recording participant exclusion criteria:** Participants whose average reaction time exceeded 500 ms would
140 have been excluded from the study (applied to zero participants). This criterion was based on the data shown in Figure 1
141 in the original study, from which we calculated that the mean reaction time for the slowest condition plus three times its
142 standard deviation resulted in 375 ms. Furthermore, we excluded participants for whom we obtained less than 75% of
143 usable EEG trials per condition of interest (300 and 75 trials, respectively), either due to early abortion of testing, or
144 due to a high number of trials rejected during the EEG data preprocessing (applied to two participants).

145 **Timeline:** Following the acceptance of first-stage preregistration, we immediately proceeded to testing participants.
146 The data collection and preregistered analyses were concluded within one and a half years.

147 **Data and Code Availability:** Due to less stringent standards for data storage at the time the original study was
148 recorded, these data are no longer available, which further motivated the replication attempt. Anonymized behavioral,
149 as well as the raw and preprocessed EEG data are available on the Open Science Framework, together with the analysis
150 code written in Matlab and R: <https://osf.io/u24tn/>.

151 **Experimental paradigm**

152 The experimental paradigm was implemented using the Psychophysics Toolbox (Brainard, 1997, Pelli, 1997) under
153 Windows 7, using a Black Box Toolkit USB response pad for response collection. Participants were instructed to use the
154 index finger of the right hand to respond. The EEG recordings took place in an electrically shielded sound-attenuated
155 EEG booth at the Center of Brain, Behavior and Metabolism (CBBM) at the University of Lübeck, Germany.

156 Participants were presented with cue-target pairs of pure tone auditory stimuli, embedded in a rhythmic stream (depicted
157 in Figure 1), and instructed to perform a speeded response to the target. Cues and targets were separated by an interval
158 of 1350 ms or 2700 ms, with an inter-trial interval of 1350 ms, such that stimulation was fully periodic at a frequency
159 of 0.74 Hz. Tones were presented via headphones at 70 dB SPL, the cue tones at 1046 and 1318 Hz, and the targets
160 at 1975 Hz. Cue tones had a duration of 150 ms, and targets a duration of 50 ms, both with 10 ms rise and fall times.
161 Crucially, the cue tone's frequency was probabilistically associated with the temporal onset of the target tone, indicating
162 whether the target is more likely to occur at the first (1350 ms), or second possible time point (2700 ms) with a 20%
163 versus 80% or 80% versus 20% probability-ratio. Short and long cue-target intervals (SOAs), and accordingly the cues
164 associated with them, were balanced with a 50/50% ratio, and presented in random order. While the original study
165 mentions no reversal of the assignment between cue frequency and target onset time over participants, we here switched
166 the assignment for every second participant. The relevance and meaning of the cues was fully disclosed to participants
167 prior to the experiment.

168 Throughout the whole experiment, participants were asked to fixate a black fixation cross on a gray background. Written
169 instructions were presented on the screen, including the information about the temporal contingencies between cue and
170 target tones. If a participant pressed the response-button before the target, a red 'x' was presented for 0.2 s. Otherwise,
171 directly after the response, the fixation cross turned white for 0.2 s to indicate that a response was registered. If no
172 response was given, a black 'x' was displayed for 0.2 s.

173 After a short training on the task (50 trials, average trial duration of 3375 ms), participants performed 1000 trials (500
174 per cue type) divided into 10 blocks. After each block, the number of missed and early trials (response prior to target
175 onset) were written on the screen, and participants took a break of minimally 60 s and continued the experiment after a
176 self-determined time. For the EEG analyses, this resulted in 100/400 trials at which unexpectedly/ expectedly no target
177 occurred at the early time point (minus outlier trials, see below).

178 **Behavioral analyses**

179 Reaction times were screened for outliers on single trials, defined as differing by more than three standard deviations
180 from the participant's mean, and removed. On average, we removed 31.23 trials per participant (SD: 12.78).

181 To decide when to stop testing (referred to as **Hypothesis 1**, p.5) we performed a paired, one-sided Bayesian t-test on
182 reaction times for targets occurring at the early time point, using the R-package *BayesFactor* (Morey and Rouder, 2018,
183 decision criterion: $BF > 10$ or $BF < 0.1$).

184 After completion of data collection, we computed a linear mixed effect model on single trial log-transformed reaction
185 times, using the *lme4* package in R (Bates et al., 2015). We modelled target occurrence (early/ late) and whether this
186 matched the expectation (expected/ unexpected) as fixed effect factors, plus their interaction. We specified random
187 intercepts and random slopes for both factors and the interaction, allowing them to vary over participants. To compute
188 p-values, we used the Satterthwaite approximation of degrees of freedom, implemented in the *lmerTest* package in R
189 (Kuznetsova et al., 2016). The α level for assuming statistical significance is set to $p < 0.02$.

190 **Hypothesis 1** was assessed by testing for a main effect of expectation on reaction times (reduced reaction times at
191 expected time points). We also expected to find an interaction of expectation and target occurrence, such that the
192 reduction of reaction times is more pronounced at the early time window.

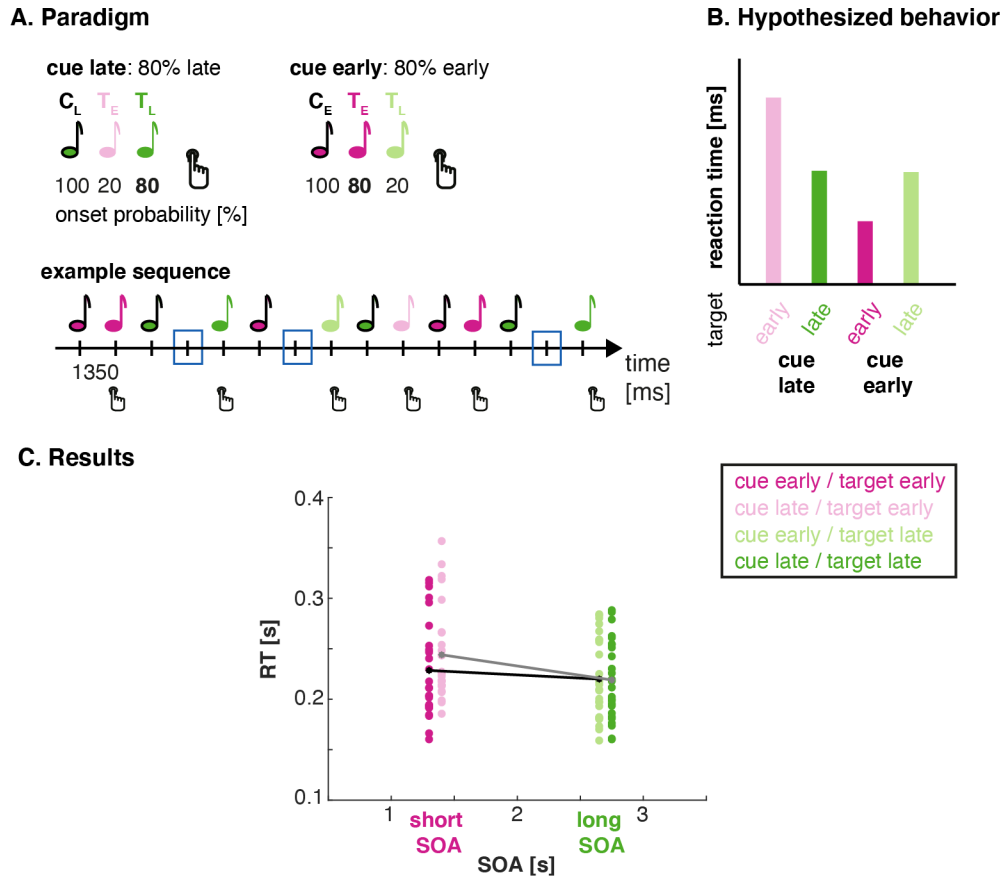


Figure 1: **A. Study Design:** Tone pairs were presented, forming a rhythmic stream. Each pair consisted of a cue (C, black contours), and a target (T, colored). Cues could be of two frequencies (1046 and 1318 Hz, indicated in pink and green), which were associated with the target's (1975 Hz) onset probability at the late (2700 ms, L) or early (1350 ms, E) time point following the cue, that is a with a 20% versus 80% or 80% versus 20% probability-ratio for a short versus long SOA. Participants were instructed to respond to the target with a button press as fast as possible. The lower panel depicts an example sequence with the time window of interest for the EEG analysis marked by blue squares. **B.** Hypothesized facilitation of reaction times by expectation: targets occurring at the expected time lead to shortened reaction times (darker bars). The effect was hypothesized to be more pronounced at the early time point (depicted in pink). **C. Results:** As predicted, reaction times to targets occurring at the short SOA were faster when the cue indicated an early target versus a late target. At the long SOA, no statistically significant difference was found between valid and invalid cues.

193 EEG recordings

194 EEG was recorded with 64 electrodes from an Acticap (Easy Cap) system, with one of the electrodes attached to the
 195 nose ¹, connected to an ActiChamp (Brain Products) amplifier using the software Brain Recorder (Brain Products).
 196 Impedance was kept below 10 k Ω . To retain the realised electrode localisation with good spatial specificity for posterity,
 197 we digitized each participant's EEG electrode positions (using the Xensor system, ANT Neuro).

198 EEG data were recorded at 1000 Hz sampling rate, without an online high-pass filter (DC), and a low-pass filter of
 199 300 Hz, contrary to the original study in which the recordings were performed with an 0.16–150 Hz analog high-pass
 200 filter.

201 After each recording, we recorded 3 minutes of EEG data with the same parameters as above, while participants listened
 202 to low-pass filtered white noise (5 kHz)². To engage participants in listening, 6 target tones (the same as in the main

¹We did not use an external electrode as originally pre-registered, because it was not compatible with the recording system.

²Originally, we had pre-registered to record 5 min, prior to the task and present 5 tones. Due to practical constraints, the block was shifted to the end of the session and shortened to 3 minutes

203 task) were presented at random intervals during the 3 min. Participants were instructed to count the tones. These data
204 were preprocessed as described below and used to test for spontaneous delta oscillations in auditory areas.

205 EEG preprocessing

206 For the preprocessing of the EEG data, we used the Fieldtrip software package (version 20200327, Oostenveld et al.,
207 2011) for Matlab (version 2019a, MATLAB, 2019). The original study used the nose as reference. In accordance
208 with our previous work, we re-referenced the data to linked mastoids using electrodes TP9 and TP10 from the cap.
209 Furthermore, we also performed a comparison analysis with the data referenced to the nose electrode, as done by the
210 original study.

211 In the original publication, a narrow delta-band filter, and a wide-band filter were applied to the data. Here, we produced
212 four parallel versions of the data, by filtering the continuous data (before epoching) with different high- and low-pass
213 filters. We chose not to apply a high-pass filter to the wide-band data to avoid temporal smearing, resulting from the
214 long filters needed to achieve low high-pass cut-offs. To test how specific the phase coherence effect is in the frequency
215 domain, we performed parallel analyses on data filtered for the low delta band (matching the stimulation frequency of
216 0.74 Hz), and for the theta band to test for a more broad-band effect that could also be influenced by evoked potentials.

- 217 1. *wide band, no high-pass filter*: <20 Hz
- 218 2. *delta band*: 0.5-3 Hz
- 219 3. *low delta band*: 0.25-1.5 Hz
- 220 4. *theta band*: 4-7 Hz

221 All filters were causal (zero-phase) FIR filters, filtering in the forward and backward directions, using the firfilt routine
222 implemented in Fieldtrip (Widmann et al., 2015). The analyses of phase consistency was performed on the delta band
223 (2), low delta band (3), and theta band (4) version of the data. The analyses of the evoked responses were performed on
224 the wide-band data (1) and the filtered versions (1 – 4).

225 Artifact rejection followed an established pipeline as used in previous studies (Herbst and Obleser, 2019), performed on
226 the wide-band filtered data (<20 Hz), and applied to all other versions of the data. First, data were visually inspected
227 to mark bad channels to be interpolated later. Then, the above filters were applied on the continuous data, before the
228 data were epoched from –500 ms before to 4050 ms after the cue stimuli. The epoched data were downsampled to
229 100 Hz to reduce computation time.³ The wide-band filtered data were detrended over the whole epoch.

230 For the ICA, we produced an additional version of the continuous data, to which we applied a 1 Hz high-pass and a
231 20 Hz low-pass filter (same filter parameters as above)⁴. The 1 Hz high pass filter was added to make the ICA solutions
232 more stable (Winkler et al., 2015), and to make the ICA blind to fluctuations at the stimulation frequency, in order to
233 avoid having to make decisions about such components during the manual selection procedure.

234 ICA was then computed on epoched data, using the 'runica' algorithm. Components reflecting blinks, muscular artifacts,
235 and unspecific noise occurring temporarily in a channel or trial were excluded, using the semi-automatic inspection of
236 ICA components provided by the SASICA toolbox for fieldtrip (Chaumon et al., 2015) and removal of these, resulting
237 in 2.19 (SD: 0.49) components removed on average per participant. Furthermore, we removed trials with voltage
238 exceeding 100 μV ⁵ (on average 35.12 trials per participant, SD: 47.90) and inspected the remaining epochs visually to
239 remove artefactual trials not detected by the above described procedure (4.58 trials on average, SD: 3.72).

240 After preprocessing, we retained on average 829.58 trials per participant (SD: 189.08).

241 EEG analyses

242 Analysis of delta phase consistency using cosine similarity

243 To assess instantaneous delta phase angles, we applied the Hilbert transform to the filtered and epoched data of the
244 different filter bands, and extracted phase angles as the imaginary value of the complex Fourier spectrum⁶. The main

³Resampling was missing in the pre-registration, but necessary to avoid too large data sets and computation times.

⁴Added after pre-registration.

⁵for one participant, the threshold was set to 150 μV , because of high-amplitude alpha oscillations, that would otherwise have resulted in rejecting many epochs

⁶We had pre-registered to apply the Hilbert transform on the continuous data, before epoching, but realized that this would make the epochs-based artefact rejection procedure obsolete. Especially the resampling and rejection of ICA components lead to transformations of the original data values, that would make the resulting phase angle time series difficult to interpret

245 analysis focuses on the delta band (0.5–3 Hz), but all other narrow-band filtered versions of the data (see above) were
 246 run through the same procedure to assess the specificity of the effects.

247 The analysis of phase consistency was performed at the time of the expected delivery of the early target, 1350 ms
 248 following the cue (indicated by blue squares in Figure 1A). We only included trials at which targets did not occur in
 249 this time window but at the later one, to keep the time window of interest free from target-evoked activity. In order to
 250 demonstrate the presence of ongoing oscillatory activity in a specific frequency range, we also display the phase-sorted
 251 single-trial data as done in in the original study (Figure 2).

252 Inter-trial phase consistency (ITC), as most commonly computed, is not independent of the number of trials (Chou
 253 and Hsu, 2018), and tends to be inflated by small trial numbers. Given the design, comparing trials in which no target
 254 occurred at the early time point when the participant expected a target to occur then (20% of trials) versus at the
 255 second time point (80% of trials) leads to an important difference in the number of trials available per cue condition.
 256 Therefore, we computed cosine similarity instead of conventional ITC measures, separately per participant, condition,
 257 and electrode, which gives an unbiased and consistent estimate of phase consistency for finite sample size (Chou and
 258 Hsu, 2018).

259 The mean cosine angle of all given pairs of phase angles (CS) per condition was computed per participant as follows
 260 with n being the number of trials, and $i, j=i+1$, being the indices of single trials compared against each other:

$$CS = \frac{2}{n(n-1)} \sum_{i=1}^{n-1} \sum_{j=i+1}^n \cos(\theta_i - \theta_j) \quad (1)$$

261 To test for a statistically significant increase in phase consistency, we compared the obtained cosine similarity values per
 262 participant at electrode Cz (used in the original study), using the paired Bayesian t-test from the R-package *BayesFactor*
 263 (Morey and Rouder, 2018, one-sided decision criterion: $BF > 10$ or $BF < 0.01$). This test was used to decide when to
 264 stop testing (**Hypothesis 2**, p.5).

265 **Hypothesis 2:** In line with the original study, we expected to find increased delta phase consistency at electrode Cz
 266 when a strong (80%) versus weak (20%) expectation existed towards the early time point.

267 After completion of data collection, and confirmation of increased delta phase consistency at electrode Cz, we computed
 268 cosine similarity values for all electrodes and subjected them to a cluster-based permutation test (Maris and Oostenveld,
 269 2007) at the group level. To assess differences in phase consistency between the early- and late-cue conditions, we
 270 computed a reference distribution of the difference between cue types using a permutation approach. To obtain the
 271 permutation distribution of the difference, we shuffled the cue types randomly over trials within each participant,
 272 keeping the ratio between numbers of early and late cues constant, and computed cosine similarity as above. This
 273 procedure was repeated 1,000 times⁷. The 98% percentile of the distribution of differences of phase concentration
 274 parameters between conditions was used as criterion to decide whether the difference in phase consistency between
 275 high and low expectation trials is different (directional test). Furthermore, the same analysis was computed on the low
 276 delta and theta band filtered data to assess the specificity of the effect to the delta range.

277 Analysis of delta phase consistency using resultant vector length

278 To match the analyses in the original study, and assess phase consistency of delta oscillations separately per condition,
 279 we computed phase concentration parameters as the resultant vector length R for all trials from one participant and
 280 condition (Berens, 2009):

$$R = \frac{\text{abs}(\sum_{n=1}^N (e^{i\cdot\theta}))}{N} \quad (2)$$

281 where θ denotes single trial phase angles in radian per condition and participant, n the number of trials from $1:N$.
 282 To statistically test for phase alignment at electrodes Cz, Fz, Pz, C3, and C4, reflected by a non-random distribution
 283 of phase angles, we tested the distribution against a van Mises distribution, applying Rayleigh’s test for uniformity
 284 of circular data, implemented in the *CircStat* package for Matlab (Berens, 2009, Fisher, 1995), for both cue types
 285 separately. We expected to see significant delta phase concentration ($p < 0.02$) in both cue conditions. As described
 286 for cosine similarity above, we also computed the resultant vector length R at all electrodes and compared it against a
 287 reference distribution obtained from permuting the cue conditions.

⁷The originally preregistered 10,000 permutations turned out too computationally intensive for the cosine similarity computation.

288 **Additional Analyses**

289 **Separating oscillatory from 1/f activity**

290 The original study assessed the presence of entrained delta oscillations by computing fast Fourier spectra (FFT) of the
291 interval -500:0 ms prior to target onset at electrode Cz. Here, we additionally assessed whether the activity observed
292 in the delta band is truly oscillatory, rather than reflecting aperiodic 1/f activity. To this end, we applied the irregular
293 resampling technique (IRASA, Wen and Liu, 2016; see also Helfrich et al., 2018, Henry et al., 2016, Herbst and Obleser,
294 2019) to the epoched data⁸, as well as to the 3-min continuous noise recording (epoched into 5-s segments to match
295 the epoch duration of the task data). The IRASA technique consists in downsampling the data at pairwise non-integer
296 values and computing the geometric mean of the resulting power spectra. The resampling leaves the 1/f activity intact
297 but removes narrow-band oscillatory activity. Power spectral density (PSD) was computed on the epochs, padded to
298 5.4 s, and in 0.19 s steps (parameters chosen to include the stimulation frequency and multiples thereof in the resulting
299 frequencies), using a fast Fourier transform tapered with a Hanning window for a frequency range of 0.19 – 22.2 Hz,
300 without detrending, and the default resampling parameter for IRASA (1.1 to 1.9, 0.05 increment).

301 To assess the presence of oscillatory activity, we subtracted the power spectrum of the re-sampled data from the power
302 spectrum of the original data, and computed a 98% confidence interval of the difference over participants using the
303 t-statistic to test for residual oscillatory activity in the delta frequency range (0.5–3 Hz).

304 To assess whether delta oscillations were present throughout the whole trial rather than resulting from periodically
305 elicited evoked responses, we masked the 300 ms after each target onset, and computed the power spectrum again (see
306 supplementary Figure 1).

307 **Hypothesis 3:** Given the rhythmic stimulation applied, we assumed to see a significant and narrow peak in the power
308 spectrum computed during blocks, which was expected at the stimulation frequency (0.74 Hz), supposedly reflecting
309 entrained oscillations.

310 **Evoked responses in the peri-stimulus time windows**

311 Evoked responses, such as the contingent negative variation (Walter et al., 1964) and P300 (Schürmann et al., 2001),
312 have been described in relation to expectation, by a literature mainly separate from the one referring to neural oscillations.
313 It is to date an open question, whether these responses relate to different or at least partially overlapping brain processes
314 (Lakatos et al., 2008, Makeig et al., 2002). Answering this question from an empirical point of view likely requires an
315 extended research program, including invasive recordings of local field potentials.

316 Nevertheless, we applied a set of additional analyses in the frequency and time-domain to better understand the nature
317 of the observed effects. In the time domain, we assessed responses to cue and target tones, from the wide-band and
318 narrow-band filtered data. Specifically, we compared the cue-evoked responses for cues predicting early versus late
319 target onsets, and the target-evoked responses for expected versus unexpected targets at the early and late time point.
320 Additionally, we compared the evoked responses in the time window of the early target onset, when no target occurred
321 then, to assess omission responses and their modulation by the strength of the expectation.

322 To test for statistically significant differences in the time-domain data, we applied cluster permutation tests on two
323 levels. First, we contrasted evoked activity for each stimulus and condition for each participant using independent
324 samples regression implemented in FieldTrip (ft_timelockstatistics). The resulting regression coefficients (betas) for
325 each time-electrode data point for the evoked responses were subjected to a group level analysis, using a dependent
326 samples t-test to contrast the betas from the subject-level analysis against zero. A permutation test (5000 Monte Carlo
327 random iterations) was performed with cluster-based control of type I error at a level of $\alpha=0.02$.

328 As in the original study, we further performed a correlation analysis, to assess the overlap between evoked responses and
329 delta phase consistency. To this end, we correlated the condition differences (expected versus unexpected) measured in
330 the time domain (post-cue and post-target) with the potential phase-consistency effects. We also assessed the partial
331 correlations of each of these measures with the reaction times, to disentangle their explanatory power. In addition to
332 the Pearson correlation values and Bayes Factors, we report percentage bend correlation coefficients (beta = 0.2), as a
333 robust measure of correlation (Pernet et al., 2013).

334 **Hypothesis 4a:** We expected to see a difference in early sensory evoked potentials between predicted and non-predicted
335 targets. The existing literature is somewhat undecided with respect to the expected directions of the ERP differences
336 (Lange, 2013), thus, we do not specify a direction here. In a previous experiment (Herbst and Obleser, 2019), we found
337 a difference in target-evoked potentials, with a more negative N1/P2 component after predicted targets.

⁸to be consistent with the delta phase analyses

338 **Hypothesis 4b:** We expect to see an omission response at the time point of the early target onset, when no target
339 occurred, with a larger amplitude on trials on which expectation was stronger. The strength of this response will likely
340 be partially correlated with pre-target delta phase consistency.

341 **Hypothesis 4c:** Correlation analyses were expected to show partial, but not full overlap between the time domain
342 signatures of expectation and delta phase consistency.

343 **Source reconstruction**

344 Since we obtained a significant difference in delta phase consistency in sensor space we visualized the source distribution
345 of delta phase consistency at the time point of the short SOA for trials in which no target occurred then. Compared
346 to the pre-registered methods, the source reconstruction pipeline was subject to slight adjustments, validated on the
347 reconstruction of delta and theta band phase coherence 300 ms after the cue and early target onset, where we expected
348 strongly phase-locked auditory activity. This validation is independent from the comparison of interest. As it turns out,
349 the cue evoked response is most strongly reflected by theta band phase coherence (see also Figure 6).

350 We used the individually digitized electrode positions, combined with a standard MRI template, and a standard head
351 model (based on the boundary-elements method) as implemented in FieldTrip (Oostenveld et al., 2003). The individual
352 electrode positions were coregistered to the MRI template by first aligning the fiducials, and second, manually aligning
353 the electrodes to the head surface. The delta-band filtered data was re-referenced to the average of all channels before
354 computing each individual's lead field matrix using a 1-cm grid resolution. We then applied dynamic imaging of
355 coherent sources (DICS, Gross et al., 2001) to construct the inverse model based on the cross spectral density computed
356 from the Fourier transformations of the band-pass filtered data (-0.5 to 4.5 s), centred at the average frequency of the
357 respective band. The dominant orientation per voxel was obtained using singular value decomposition. We then applied
358 the precomputed filters to the analytic representation of the single trial data (obtained through the Hilbert transform) via
359 matrix multiplication.

360 Cosine similarity was computed on single voxels, to visualize the distribution of delta phase consistency per condition.
361 We computed a t-test between cues indicating early versus late targets, using the Montecarlo permutation method
362 (ft_sourcestatistics). Since the source reconstruction was performed to localize the findings at the sensor level and not
363 as an independent statistical test, we display the T-values thresholded at, $p < 0.02$ (non-parametric permutation test)
364 without any further correction for multiple comparison (Figure 2D, H). Source labels are reported based on the AAL
365 atlas (Tzourio-Mazoyer et al., 2002).

366 While we have shown in previous work that auditory and motor-like sources can be broadly distinguished by recon-
367 structing source activity from EEG data (Herbst et al., 2018), the identification of the exact anatomical generators will
368 require further confirmation by follow-up studies, for instance using MEG.

369 **Hypothesis 5:** We expected to see the strongest delta phase consistency in auditory and motor areas (Morillon et al.,
370 2019, Morillon and Baillet, 2017).

371 Results

372 Expectations speed up reaction times

373 In line with Hypothesis 1, reaction times were affected by the predictions conveyed by the cues (see Figure 1). At
374 the short SOA, responses to validly cued targets were faster than responses to invalidly cued targets (valid: 0.229 s,
375 SD = 0.048 s, invalid: 0.244 s, SD = 0.046 s; significant difference: $t(25) = 5.42$, $p < 0.001$, Bayes Factor (BF) = 3464.96;
376 one-sided tests performed on log-transformed reaction times). Furthermore, we found the hypothesized interaction,
377 namely no significant difference in reaction times at the long SOA (validly cued: 0.219 s, SD = 0.039 s, invalidly cued:
378 0.220 s, SD = 0.039 s; $t(25) = 1.28$, $p = 0.11$, BF = 0.76).

379 The linear mixed effect model computed on single trial log transformed reaction times confirmed that both factors, SOA
380 and cue validity were significant, as well as their interaction (see Table 1).

	F value	p value
cue validity	$F(1, 24.97) = 28.80$	< 0.001
SOA	$F(1, 24.98) = 14.64$	< 0.001
cue validity \times SOA	$F(1, 24.89) = 20.92$	< 0.001

Table 1: **Statistical results of the reaction time analysis.** A linear mixed effect model revealed significant main effects of cue validity and SOA, as well as a significant interaction.

381 Delta phase consistency increases with expectation for target occurrence

382 In confirmation of Hypothesis 2, we observed increased delta phase coherence at electrode Cz at the time point of the
383 early SOA when the cue predicted an early versus a late target (cosine similarity, cue early: 0.09, cue late, 0.04, $T(25) =$
384 2.67 , $p = 0.006$, BF = 7.40). In the low delta band, the effect was even stronger, as indicated by the larger absolute
385 difference and Bayes Factor (cosine similarity, cue early: 0.13, cue late, 0.05, $T(25) = 2.30$, $p = 0.003$, BF = 14.37).

386 The phase-sorted single trial amplitude time courses depicted in Figure 2A and E (displayed to match the original study)
387 show that across all participants 40.6% of cue early trials had a delta phase angle of $-\pi/2$ and $\pi/2$ at the early SOA,
388 considered the less favourable phase, versus 43.7% in the cue late condition (38.8% versus 43.0% for the low delta
389 band).

390 Cluster permutation tests comparing the difference in cosine similarity between cue early and cue late trials at all
391 electrodes against the difference obtained from permuting trials between the two conditions revealed significantly
392 increased phase consistency in the delta and low delta bands, but not in the theta band (see Figure 2, statistics reported
393 in Table 2). The analysis of resultant vector length found similar results.

394 The cluster permutation analysis takes into account the difference in the number of trials per condition (cue early: 20%,
395 cue late: 80%), as the trial numbers were kept consistent when computing the permuted differences. As can be seen in
396 Figure 2 B, D (and panels F, G, for the low delta band), cosine similarity was not inflated for the condition with fewer
397 trials (the grey dots indicating the permuted difference lie on the unity line), while for resultant vector length there was
398 an inflation (grey dots lie beyond the unity line).

399 We performed a control analysis with the nose electrode as the reference to match the original study, which yielded a
400 weaker increase in phase consistency for the cue early condition (delta band: cosine similarity, cue early: 0.08, cue late,
401 0.04, $T(25) = 2.02$, $p = 0.027$, BF = 2.31; low delta band: cosine similarity, cue early: 0.16, cue late, 0.06, $T(25) = 3.60$,
402 $p = 0.004$, BF = 12.26). The decrease in effect size might be explained by the fact that the recording from the nose
403 electrode turned out to be rather noisy in many participants.

404 Source reconstruction of delta and low delta phase consistency (cosine similarity; Figure 2 D, H) showed mainly
405 pre-motor and motor sources, extending into frontal areas, as well as anterior temporal and auditory areas. In the delta
406 band, the difference between the cue-conditions was most apparent in temporal areas (middle and inferior temporal
407 gyrus, predominantly in the left hemisphere), and somewhat weaker in (pre-)motor areas (right supplementary motor
408 area). In the low delta band, the strongest difference occurred in (pre-)motor areas (supplementary motor areas, stronger
409 in the right hemisphere), extending into frontal areas. Weaker differences were observed in parietal and temporal areas.

410 In line with the original study, we also tested whether the phase distributions in the delta band were randomly distributed
411 or concentrated, as a signature of entrainment. Significant delta phase concentration at the early SOA was observed
412 at electrode Cz in 13 out of 26 participants for the cue early condition, and 18 participants in the cue late condition
413 (p -values < 0.02 ; Fz: 10/14, C3: 12/15, Pz: 10/12, C4: 12/14). For the low delta band, 17 participants had a significant

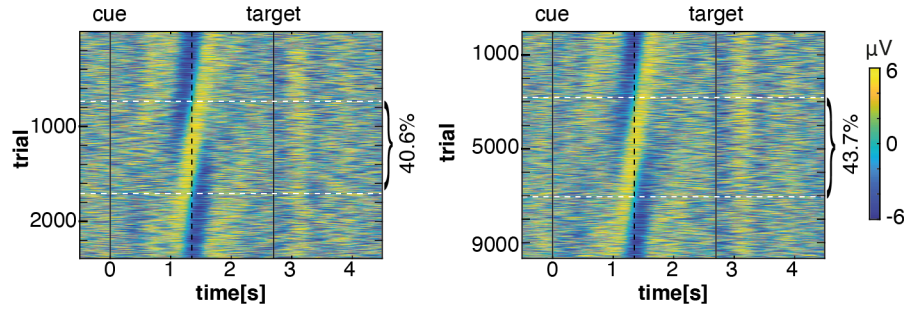
414 phase concentration at electrode Cz in the cue early and 20 in the cue late condition (p-values < 0.02; Fz: 15/14, C3:
415 13/20, Pz: 15/21, C4: 18/16). These results suggest oscillatory entrainment in the majority, but not in all participants.
416 Additionally (not part of the pre-registration), we visualized phase locking values over time for the two SOAs and
417 two cue conditions, for the delta, low delta, and theta band (see Figure 6). Interestingly, delta and low delta phase
418 consistency showed a transient increase after targets, but much less after cues, while evoked responses at the cue and
419 target lead to a prominent increase in theta phase consistency. A prolonged difference at the early SOA between cues
420 indicating early versus late targets (green lines) occurred in the delta and low delta band, as already apparent in the
421 previous results.

frequency		mean (Cz) cue early	mean (Cz) cue late	cluster p-value
low delta	cosine similarity	0.13	0.05	p < 0.001
	resultant vector length	0.23	0.15	p = 0.003
delta	cosine similarity	0.09	0.04	p = 0.001
	resultant vector length	0.20	0.13	p = 0.005
theta	cosine similarity	-0.01	0.01	no positive cluster found
	resultant vector length	0.08	0.05	no positive cluster found

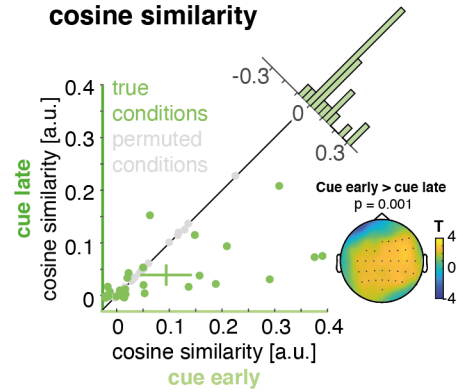
Table 2: **Statistical results of the phase consistency analyses.** The average phase consistency across participants is reported for the two measures: cosine similarity and resultant vector length, both for electrode Cz. Cluster permutation tests comparing the difference in phase consistency between cue early and cue late trials at all electrodes against the difference obtained from permuting trials between the two conditions revealed significantly increased phase consistency in the low delta and delta band for both measures, but not in the theta band.

Figure 2: (Figure on next page.) **A. Delta band (0.5 – 3 Hz), phase-sorted amplitude time courses:** This display was included for better comparison with the original study (their Figure 3E, F) and shows all trials of all participants, for the long SOA, with cues indicating an early target in the left panel, and cues indicating a late target in the right panel. The band-pass filtered single trials were sorted by phase angle at the early SOA. The range between the horizontal white lines, demarcating phase angles between $-\pi/2$ and $\pi/2$, is considered the less favourable phase. The proportion of trials in that phase range is smaller in the cue early condition (40.6%), compared to the cue late condition (43.7%). **B. Delta phase consistency: cosine similarity:** Phase consistency was higher in the cue early condition, indicated by most green dots lying beyond the diagonal line. Grey dots depict phase consistency values computed after permuting trials randomly between conditions. The topography shows the significant cluster when comparing phase consistency between the true conditions and the resampled version. The histogram above the diagonal depicts the differences cue early – cue late. **C. Delta phase consistency: resultant vector length:** As in B, but here phase consistency was measured by resultant vector length. The departure of the grey dots from the diagonal indicates a systematic overestimation of phase consistency by this measure for the condition with fewer trials. Nevertheless, the comparison between true and permuted conditions showed a significant cluster. **D. Source reconstruction.** Average cosine similarity values at the short SOA are shown overlaid on a template brain, for cue early and cue late conditions separately (note the different color scales). The third panel shows the difference between cue early and cue late with the colors scale indicating T-values thresholded at $p < 0.02$ (non-parametric permutation test) with no further correction for multiple comparisons. In the delta band, the difference in phase-locking was strongest in temporal (auditory) areas, as well as pre-motor and motor areas. **E–H: Low delta band (0.25 – 1.5 Hz).** Same as A – D, but for the low delta band. Phase consistency in the low delta band was significantly higher after cues indicating an early versus late target, with a pattern very similar to the results observed in the delta band. In source space, the difference was most pronounced in pre-motor and motor areas, but also occurred in temporal and parietal areas.

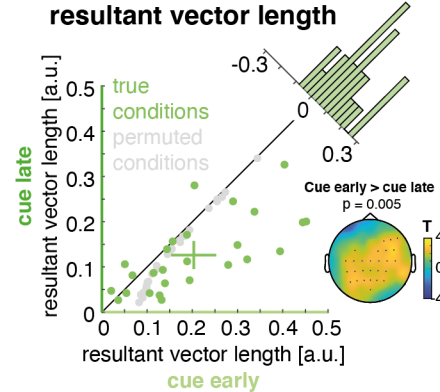
A) Delta band (0.5 – 3 Hz): single trial amplitudes, phase-sorted
cue early (Cz) cue late (Cz)



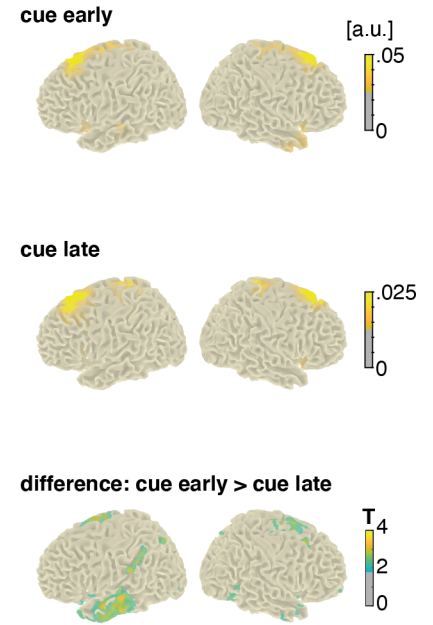
B) Delta phase consistency: cosine similarity



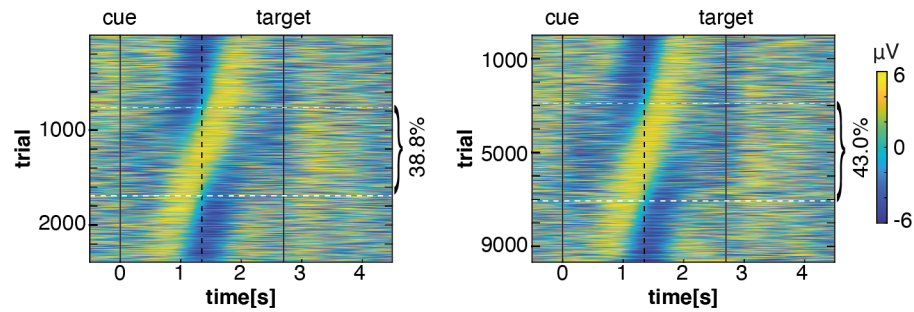
C) Delta phase consistency: resultant vector length



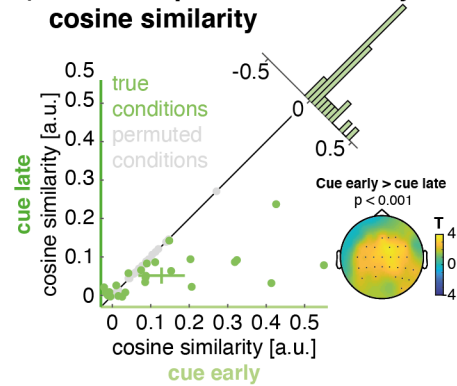
D) Source reconstruction: cosine similarity delta band



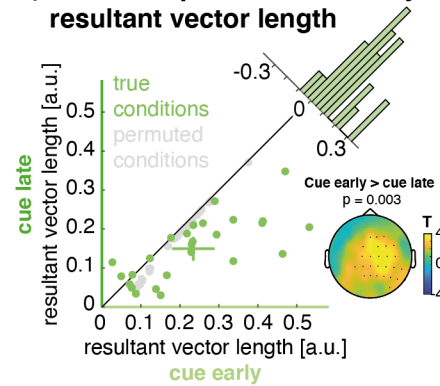
E) Low delta band (0.25 – 1.5 Hz): single trial amplitudes, phase-sorted
cue early (Cz) cue late (Cz)



F) Low delta phase consistency: cosine similarity



G) Low delta phase consistency: resultant vector length



H) Source reconstruction: cosine similarity low delta band

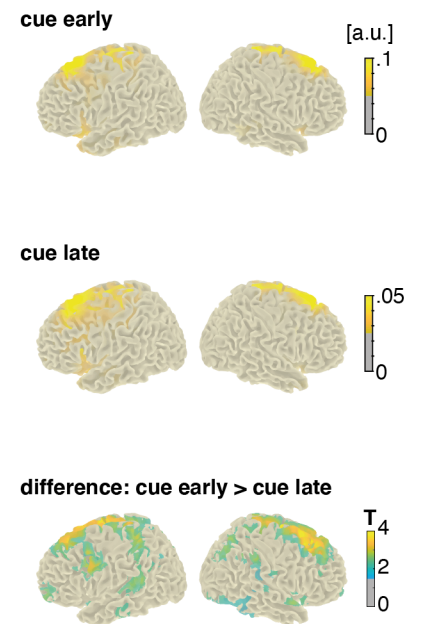


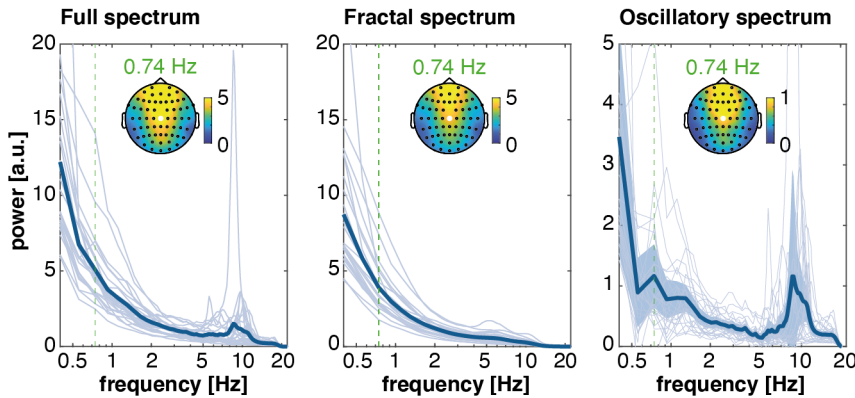
Figure 2: Caption on previous page

423 **Power spectra show peaks at the stimulation frequency**

424 We assessed the power spectra of the data recorded during the task and the subsequent block in which participants
425 listened to white noise (Figure 3). After removal of the 1/f slope, the oscillatory spectrum contained a peak at the
426 stimulation frequency (0.74) at fronto-central electrodes in the task data (Figure 3A), but not in the resting state data
427 (Figure 3B). The peak indicates an oscillation evoked by the rhythmic stimulation, and confirms Hypothesis 3. Note that
428 the seemingly larger rise at around 0.3 – 0.4 Hz reflects the cut-off in the power spectrum caused by the epoch duration
429 (5 s), preventing us from computing power at the lowest frequencies.

430 After removing the target-evoked responses (0 – 300 ms after each target), power spectra still showed a peak at the
431 stimulation frequency, albeit with slightly reduced power (shown in Supplementary Figure 1).

A) Power spectra: task (Cz)



B) Power spectra: resting state (Cz)

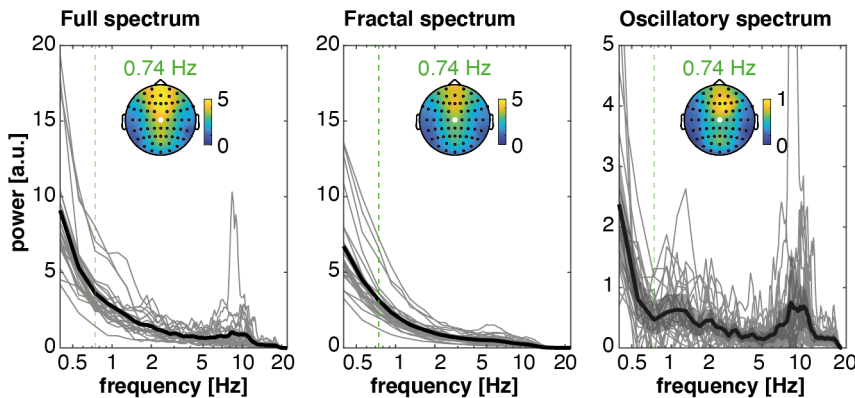


Figure 3: **Power Spectra.**

A) Power spectra of the task data, all at electrode Cz. Left: Full power spectrum. Middle: Fractal power spectrum, computed using the irregular resampling technique. Right: Oscillatory spectrum, computed as the difference between the full and fractal spectra. Thick lines depict participant average, thin lines single participants' spectra. The blue shade in the right panel depicts the 98% confidence interval. The green dotted vertical line indicates the stimulation frequency (0.74 Hz). The topographies show the scalp distribution of power at 0.74 Hz. **B) Power spectra of the resting state.** Panels: as in A. While the power spectra computed on the task data showed a peak at the stimulation frequency, the resting state data did not show a clear peak.

432 **Evoked responses show stronger pre-target deflections towards predicted early targets, and post-target**
 433 **differences in the delta band**

434 We observed clear auditory evoked responses to cue and target tones, as well as a negative deflection following the cue
 435 (see Figure 4). In the long SOA trials, a delta-like wave form was observed at central electrodes.
 436 Contrary to Hypothesis 4a, we observed no statistically significant differences in the evoked responses to expected and
 437 unexpected targets in the wide-band data (0 – 20 Hz, Figure 4A, see also Table 3). In the delta-band filtered data (0.5 –
 438 3 Hz, Figure 4B), we observed a stronger response to expected early targets (cue early) compared to unexpected early
 439 targets (cue late; 1.48 – 1.84 s, $p < 0.01$). No significant effects were found for the late target trials ($p < 0.14$).
 440 As specified in Hypothesis 4b, we expected to see an omission response in trials for which the cue predicted an
 441 early target but none appeared, defined as an evoked-like potential in the post-target window (Dercksen et al., 2020,
 442 SanMiguel et al., 2013). No such response was observed, neither in the wide-band nor the delta-band data.
 443 However, the cue-evoked responses were indicative of the prediction conveyed by the cue: in the wide band data, we
 444 observed a more negative-going slow wave towards the early SOA when the cue predicted an early target (early target
 445 trials: 1.20 – 1.37 s, $p < 0.01$; marginal for the late target trials: 1.16 – 1.29 s, $p = 0.03$). In the delta-band data, the
 446 post-cue difference was not significant (early target trials: 1.19 – 1.4 s, $p = 0.079$).
 447 Evoked responses in the low delta band and theta band data showed no significant differences (low delta $p > 0.06$; theta
 448 $p > 0.03$).

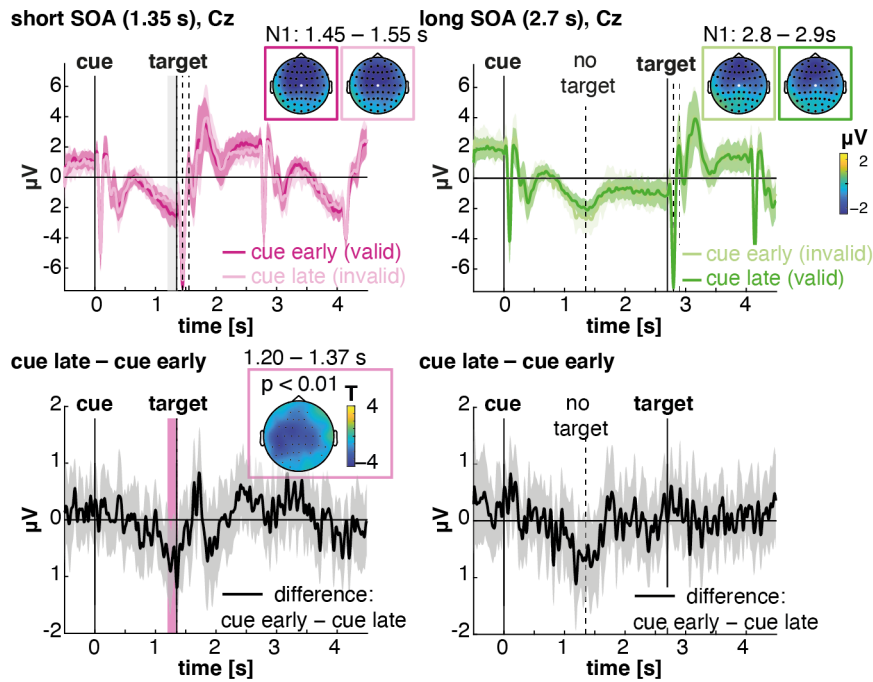
filter	SOA	latencies	direction	cluster p-value
wide band	1.35 s	1.20 – 1.37 s	neg	p < 0.01
	2.7 s	1.16 – 1.29 s	neg	p = 0.03
delta band	1.35 s	1.48 – 1.84 s	pos	p < 0.01
	2.7 s	1.19 – 1.4 s	neg	p = 0.08
low delta band	1.35 s	1.02 – 1.39 s	neg	p = 0.06
theta band	1.35 s	0.99 – 1.04 s	pos	p = 0.09

Table 3: **Statistical results of the evoked response analysis.** Findings are reported per filter band and SOA at which the target was presented. The latencies indicate the duration of the significant clusters time-locked to the cue. As for the direction, 'neg' means that the evoked activity was smaller (or more negative) following cues which predicted an early compared to late target. For 'pos' the direction is reversed.

449 **Reaction time facilitation by valid cues correlates with delta phase consistency**

450 We tested for correlations of the reaction time facilitation by valid cues and the difference in delta phase consistency
 451 (and evoked responses, respectively) across participants (see Table 4 and Figure 5). The difference in log-transformed
 452 reaction times at the short SOA correlated significantly (albeit only marginally for the robust correlations) with the
 453 difference in delta phase consistency (cosine similarity) measured at the short SOA (taken from the long SOA trials as
 454 in the previous analyses, electrode Cz: $\rho = -0.56$, robust correlation -0.29). In the low delta band, the correlation
 455 was significant, too ($\rho = -0.56$, robust correlation -0.56), see Figure 5A). The negative correlation indicates that
 456 participants who showed greater reaction time benefits from valid cues at the early SOA also had stronger delta phase
 457 consistency around the early SOA when the cue predicted an early versus late target.
 458 The reaction time facilitation did not significantly correlate with the observed differences in the slow negative potentials
 459 following the cue (wide-band data, 1.20 – 1.37 s post-cue, $\rho = 0.27$, Figure 5B, left). However, we observed a correlation
 460 between the difference in reaction times and the difference in the delta band evoked response at the early target (1.48 –
 461 1.84 s post-cue, $\rho = -0.63$, robust correlation -0.71 , Figure 5B, right), indicating that participants who responded faster
 462 to validly compared to invalidly cued targets also showed larger differences in the evoked response to those targets.
 463 No significant correlations were observed between the differences in delta phase consistency and evoked responses
 464 (Figure 5C).
 465 We also computed partial correlations between the differences in reaction times, the differences in delta phase consis-
 466 tency, and differences in the evoked response (slow negativity observed in the wide-band data). When controlling for
 467 the evoked response, the correlation between phase consistency and reaction times dropped to $\rho = -0.39$ ($p = 0.05$).
 468 When controlling for phase consistency, the correlation between the evoked response and reaction times dropped to $\rho =$
 469 0.23 ($p = 0.28$). It is important to mention here that the reaction times and evoked responses were both taken from short
 470 SOA trials, while the cosine similarity measures were computed from long SOA trials.
 471 The original study reported correlations between the phase of the delta oscillation at target onset with reaction times,
 472 as well as the latency and peak amplitude of the P300 component of the evoked response, taken from single trials in
 473 Experiment 1 (slightly different experimental design). All measures were taken at the same SOA and from single trials.

A) Evoked responses, wide band (0 – 20 Hz)



B) Evoked responses, delta band (0.5 – 3 Hz)

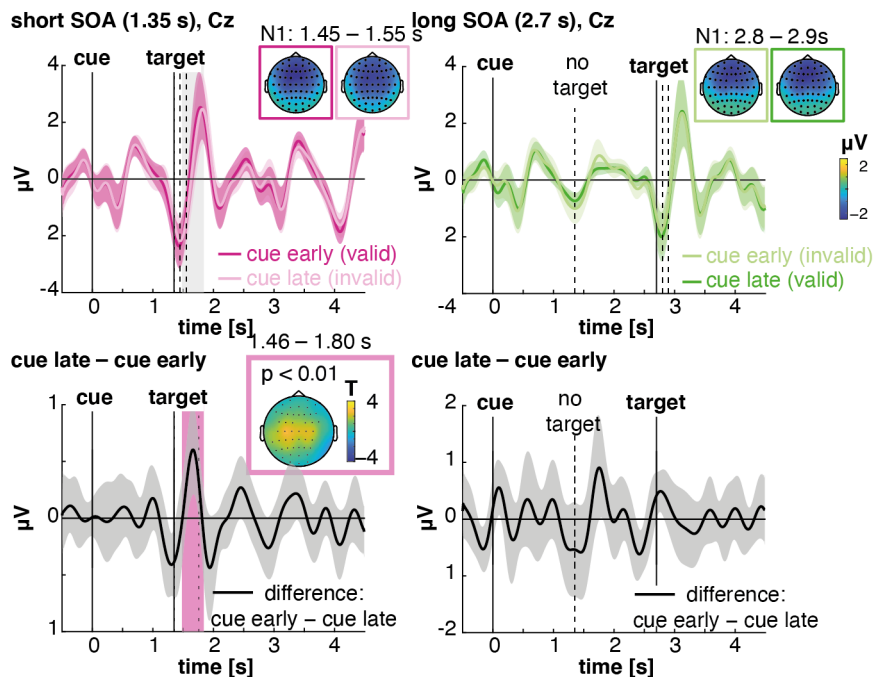


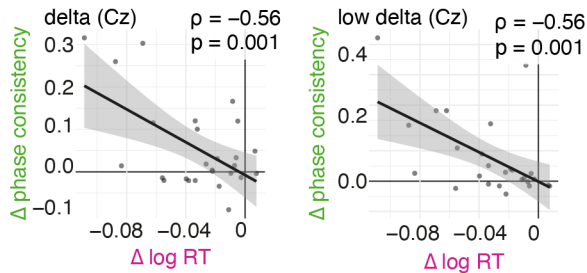
Figure 4: A. Evoked responses, wide band: Average evoked responses, time-locked to the cue at electrode Cz. Top, left: short SOA (1.35 s). Activity evoked by cues predicting early targets (valid, dark pink) versus cues predicting late targets (invalid, light pink). Top, right: long SOA (2.7 s). Activity evoked by cues predicting early targets (invalid, light green) versus cues predicting late targets (valid, dark green). The topographies show activity in the N1 time window, 100 – 200 ms after the target onset (indicated by the vertical dashed lines). Bottom row: Differences between early and late cues for the early (left) and late SOA trials (right). In the early-SOA trials, a significantly more negative potential was observed following cues predicting an early target. The pink shade indicates the time window in which a significant difference was found between the two conditions, accompanied by the topography of the statistically significant cluster. A similar pattern was found for the long SOA trials, but the difference was not statistically significant. Strictly speaking, the observed pre-target difference does not confirm the original Hypothesis 4a, which predicted *post-target* differences in the broad band data. **B. Evoked responses, delta band:** Same as in A, but for the delta-band filtered data. A larger target-evoked response occurred after expected versus unexpected early targets (left column). No differences were found in the pre-target window.

474 Here, we computed correlations between the differences in the respective measures and at different SOA, which might
 475 explain why we did not find consistent correlations between phase consistency and evoked responses.

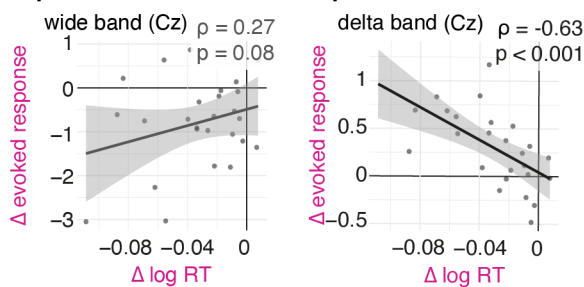
variables	ρ	T value	p-value	Bayes Factor
RT/ cosine similarity (delta)	-0.56 (-0.29)	T(24) = -3.32	0.001 (0.08)	32.65
RT/ cosine similarity (low delta)	-0.56 (-0.56)	T(24) = -3.35	0.001 (0.001)	34.81
RT/ evoked response (post-cue, wide band)	0.28 (0.11)	T(24) = 1.43	0.08 (0.30)	1.68
RT/ evoked response (post-target, delta band)	-0.63 (-0.71)	T(24) = -4.00	< 0.001 (< 0.001)	117.01
cosine similarity (delta)/ evoked response (post-cue, wide band)	-0.244 (-0.14)	T(24) = -1.23	0.11 (0.25)	1.33
cosine similarity (low delta)/ evoked response (post-cue, wide band)	-0.37 (-0.16)	T(24) = -1.98	0.03 (0.22)	3.53
cosine similarity (delta)/ evoked response (post-target, delta band)	0.18 (0.09)	T(24) = 0.87	0.20 (0.33)	0.90

Table 4: **Statistical results of the correlation analyses.** All tests are one-sided. The ρ and p-values in brackets indicate percentage bend correlation coefficients, a robust correlation estimate.

A) Correlation of response times & phase consistency



B) Response times & evoked response



C) Evoked response & phase consistency

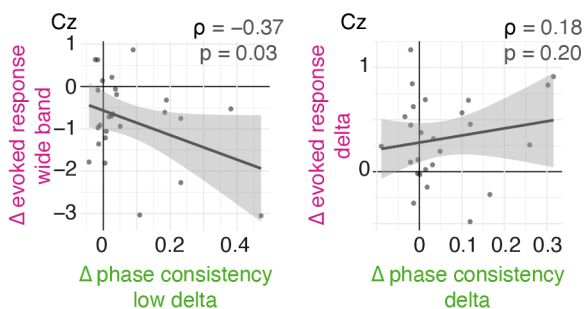


Figure 5: **Brain-behaviour correlations.** **A) Correlation between reaction times and phase consistency** for the delta band (left) and low delta band (right). Participants who had a larger difference in reaction times after expected versus unexpected early targets also had a larger difference in cosine similarity at the early SOA following early versus late cues. **B) Correlation between reaction times and evoked responses.** No significant correlation was observed between reaction times and the difference in the post-cue negativity observed in the wide band data (1.20 – 1.37 s post-cue, right panel). Participants who had a larger distance in reaction times also had a larger difference in the delta-band evoked responses to expected versus unexpected early targets (1.48 – 1.84 post-cue, left panel). **C) Correlation between evoked responses and phase consistency** for the delta band. No significant correlation was observed, neither between the slow negative difference in the wide-band data and delta phase coherence (left panel), nor between the post-target difference in the delta band data and delta phase coherence. The colors of the axis labels indicate whether the measure was taken from short (pink) or long SOA (green) trials.

476 Discussion

477 In this study, we set out to replicate the seminal findings
478 reported by Stefanics et al. (2010, Experiment II), namely
479 an increase in phase consistency of the delta oscillation
480 with the expectation for a target onset in the upcoming
481 cycle of an ongoing rhythm. All major findings of the
482 original study were replicated. We found a consistent
483 reduction of reaction times following validly cued versus
484 invalidly cued early targets by about 15 ms, confirming
485 **Hypothesis 1** (see also Figure 1). A robust effect of
486 increased delta phase consistency with expectation was
487 observed, confirming **Hypothesis 2** (see also Figure 2).
488 Additional analyses suggest that the increase in phase
489 consistency results from oscillatory entrainment rather
490 than reflecting an evoked response.
491 Concerning the more exploratory hypotheses spelled out
492 in the pre-registration, we observed a spectral peak at
493 the stimulation frequency (**Hypothesis 3**, Figure 3), and
494 sources for the phase consistency difference predominantly
495 in pre-motor, motor, and in temporal areas (Figure
496 2). The findings for the evoked responses did not ad-
497 here fully to the spelled out hypotheses: no post-target
498 differences were observed in the wide-band data with
499 respect to expectancy (**Hypothesis 4a**), but a stronger
500 response to expected targets was observed in the narrow-
501 band delta evoked response (Figure 4). Furthermore,
502 we observed, in the time window following the cue, a
503 stronger negative CNV-like deflection when the cue pre-
504 dicted an early target (Mento, 2013, Praamstra et al.,
505 2006). However, no omission response was observed in
506 the time window following unexpected omissions of the
507 early target (**Hypothesis 4b**). Brain-behavior correlations
508 were observed between reaction times and delta phase
509 consistency, as well as responses evoked by early targets
510 (**Hypothesis 5**).

511 Oscillatory phase locking as a mechanism for prediction

512 Importantly, the replication, in line with the original study, shows that delta oscillatory phase is under endogenous or
513 top-down control, allowing for an increase in phase consistency with an expectation set by the preceding cue (80%
514 versus 20% probability for target occurrence, see also Figure 2). The correlations observed between reaction times and
515 phase consistency further underline the behavioral relevance of the phase locking (Figure 5A). Together, these findings
516 strengthen the cognitive role of phase entrainment as a means to align slow neural oscillations to external temporal
517 regularities to enhance the processing of task-relevant inputs (Arnal and Giraud, 2012, Jones, 2018, Schroeder and
518 Lakatos, 2009).

519 With the increasing popularity of the theory of entrainment, criticisms have also emerged. In particular, a crucial
520 premise for entrainment in the narrow sense is the existence of an endogenous oscillation that is entrained by exogenous
521 inputs (Lakatos et al., 2019, Obleser and Kayser, 2019). Opposing views suggest that the observed phase consistency, at
522 least in some studies, could be conflated with stimulus evoked responses occurring *after* the sensory event (van Diepen
523 and Mazaheri, 2018, Zoefel and Heil, 2013), rather than oscillatory phase locking in anticipation of the stimulus.
524 Especially for low frequent oscillations, this distinction is difficult to make due to signal processing constraints (for
525 successful examples see the review by Zoefel et al., 2018).

526 Here, we conducted several additional analyses, which in our view support the interpretation of the effects as
527 oscillatory phase locking, rather than an evoked response. First, delta phase consistency at the expected target
528 onset increased in a narrow frequency band, most strongly in the low delta band which captured the ongoing
529 rhythmic stimulation (0.74 Hz), as well as the delta band, but not in the theta band. The frequency-specificity
530 strengthens the proposed role of delta phase for endogenous predictions (see also Saleh et al., 2010). The
531
532

Phase consistency time courses

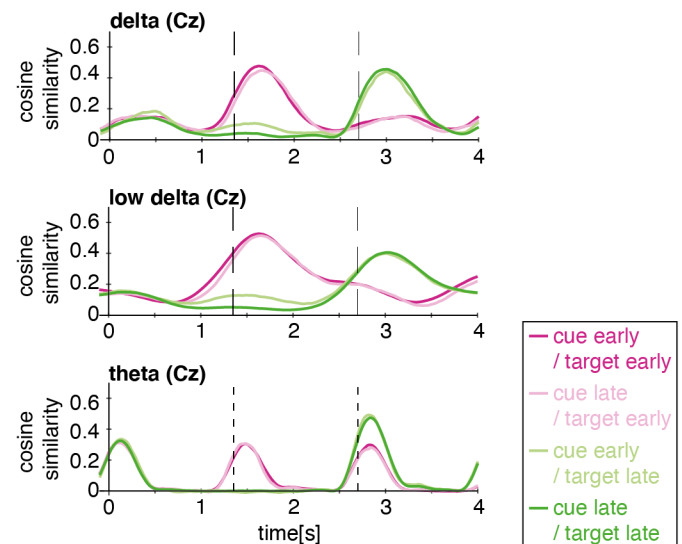


Figure 6: **Phase consistency time courses** per SOA and cue condition. Top: delta band, middle: low delta band, bottom: theta band. Targets lead to transient post-stimulus increases in phase consistency in the delta, low delta, and theta bands, but only the theta band shows a substantial increase in phase consistency following the cue. Only the delta and low delta band show a prolonged increase in phase consistency in line with an oscillatory response, and a difference at the early SOA between cues indicating early versus late targets (green lines). The time points of possible target onsets (short and long SOA) are indicated by the vertical dashed lines.

533 phase-locking time courses for the three bands (depicted in Figure 6) further emphasize this point: delta and low delta
534 phase was consistently increased throughout the trial in line with an oscillation and increased transiently only after
535 targets, while theta phase consistency increased transiently after all auditory events, likely capturing the evoked response.
536

537 Second, we observed a peak at the stimulation frequency in the power spectrum after removing the 1/f activity
538 (Figure 3), further supporting an oscillatory response. Interestingly, the oscillatory power spectra during rest also show
539 a rather broad peak around 1–1.5 Hz, which could be indicative of spontaneous oscillations in the delta band serving as
540 the basis for entrainment (Morillon et al., 2019). Further research will be needed to assess whether those peaks reflect
541 spontaneous oscillations versus artefactual activity such as the heart beat.
542

543 Third, as to the overlap between evoked responses and delta phase consistency, the picture remains somewhat unclear.
544 We did observe a pre-target difference in the wide-band data, interpretable as a stronger contingent negative variation
545 (CNV) towards early and expected targets (Figure 4A). However, we did not observe a significant correlation between
546 this difference and the response times or the delta phase consistency effect (correlations remain inconclusive as indicated
547 by the Bayes Factors; see also Figure 5B, C, left panels). We also did not observe any significant omission responses at
548 the time point of an expected early target (Dercksen et al., 2020, SanMiguel et al., 2013), ruling out that the increased
549 phase consistency observed at this moment reflects a transient evoked response.

550 The post-target difference in the delta band evoked response did correlate with response times (Figures 4B, 5B, C, right
551 panels), but not with the delta band consistency effect (both measures came from different sets of trials, namely early
552 and late target onsets, respectively). Overall, the difference in neural dynamics with respect to expectation seems best
553 captured by the phase of a narrow-band oscillation matching the frequency of the stimulation.
554

555 Admittedly, the present design cannot fully disentangle whether the delta oscillation whose phase locks to the
556 stimulation is an a-priori existing endogenous oscillation, or an oscillation that emerges in response to the rhythmic
557 stimulation. We observed an oscillatory peak during the rhythmic stimulation, but not during a block in which
558 participants listened to white noise without rhythmic stimulation (Figure 3), suggesting that the oscillation emerged in
559 response to the rhythmic stimulation. Even though the propensity of neuronal assemblies to spontaneously oscillate in
560 the delta frequency range has been shown with intra-cranial recordings (Buzsáki and Draguhn, 2004, Halgren et al.,
561 2018, Lakatos et al., 2005, Neymotin et al., 2021), this proof is difficult to achieve with non-invasive M/EEG recordings.
562 In order to test whether the implementation of predictions through phase locking occurs specifically in the delta band or
563 could occur in a wide range of frequencies, future studies could vary the stimulation frequency (see Zalta et al., 2020,
564 for a behavioral paradigm), or include longer periods of stimulus omissions to test for the continuity of an endogenous
565 oscillation (Saber and Hickok, 2021, Zoefel et al., 2018).
566

567 The increase in delta phase consistency with an endogenous expectation is an important argument for an active role
568 of neural oscillations in tracking and anticipating rhythmic sensory inputs. By entraining in period and phase to an
569 external input, neural oscillations can implement temporal predictions, allowing to align brain states beneficial for the
570 processing of the respective inputs with the predicted onsets (Arnal and Giraud, 2012, Jones, 2018, Schroeder and
571 Lakatos, 2009). Given the strictly periodic stimulus sequence used here, there are two possible interpretations for the
572 nature of the expectation: it could either be *temporal*, directed to the most likely time point of target occurrence, or
573 *probabilistic*, directed to the first or second cycle of an externally driven oscillator whose period mechanistically defines
574 the cycle duration. To further examine whether neural oscillations implement temporal predictions, variations of the
575 period of the stimulation are necessary.
576

577 Another open question currently is how much divergence from isochrony an oscillatory implementation of temporal
578 prediction can afford (see also Obleser et al., 2017). While slight variations in the period have shown to be accounted
579 for (Cannon, 2021, Doelling and Assaneo, 2021, Herrmann et al., 2016, Lakatos et al., 2013), recent research suggests
580 that temporal predictions based on single intervals might rely on at least partially diverging mechanisms (Bouwer et al.,
581 2020, Herbst and Obleser, 2017, 2019, Lange, 2013).
582

583 **Novel aspects of the current study**

584 We reconstructed the sources of the delta phase consistency effects, found to be predominantly in (pre-)motor areas, but
585 also in parietal and temporal (anterior temporal and auditory) areas, which is in line with Hypothesis 5 (Figure 2).
586 Interestingly, the difference in the delta band was stronger in the temporal and somewhat in parietal areas, while the
587 difference in the low delta band (most specific to the stimulation frequency) was strongest in pre-motor and motor areas,
588 extending into frontal and parietal areas.
589

590 This dominant localization of delta phase locking to (pre-)motor areas is in line with the assumption that rhythmic
591 activity emerging from motor areas entrains auditory cortices to rhythmic inputs (based on Morillon and Baillet, 2017,
592 Rimmele et al., 2018). However, we would like to mention that the strongly time-locked activity in bilateral auditory
593 areas might pose a challenge for source reconstruction notably when using beamformers (Hincapié et al., 2017, Popov
594 et al., 2018). In combination with the limited spatial resolution of EEG, this might have lead to an under-representation
595 of the auditory sources here. Follow-up studies using MEG could provide additional insights on the precise location of
596 the anatomical generators.

597

598 In the low delta band, weak effects were observed in parietal regions, suggested to play a role in attentional processing
599 more generally, and temporal prediction in particular (Besle et al., 2011, Coull et al., 2013). The difference to previous
600 studies here probably results from the rhythmic paradigm (Coull et al.: interval-based predictions), and the reduced
601 spatial resolution of EEG compared to functional magnetic resonance imaging (fMRI) and electrocorticography (ECoG
602 in Besle et al.).

603

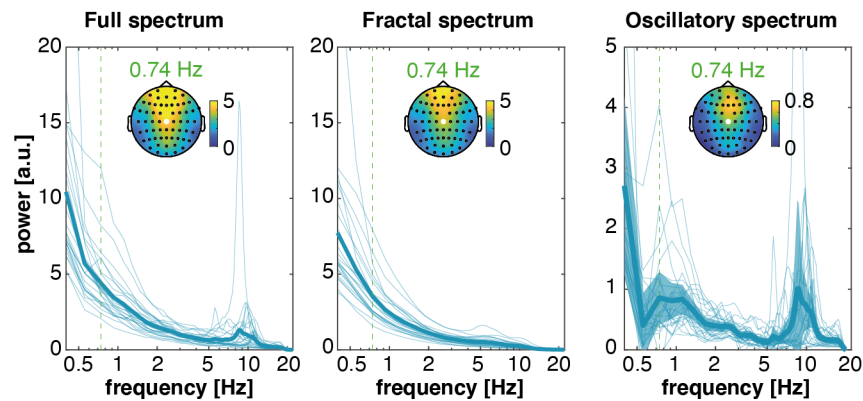
604 An important methodological aspect of the study is that by design, conditions with 20% versus 80% of trials are
605 compared, as a consequence of the manipulation of cue validity. This imbalance is particularly important when
606 comparing phase consistency between conditions, as the commonly used measures for phase locking across trials
607 (Bruns, 2004, Lachaux et al., 1999, Tallon-Baudry et al., 1996) have shown to be inflated for small number of trials
608 (Cohen, 2014, Edwards et al., 2009). In this replication, we computed cosine similarity (Chou and Hsu, 2018),
609 confirming its interpretation as an unbiased alternative to measure phase locking. This is particularly apparent in
610 the bias observed in the measure of resultant vector length towards the condition with fewer trials after permutation
611 (indicated by the grey dots in 2C, G), which we did not see in cosine similarity (Figure 2B, F).

612

613 **Conclusions**

614 In sum, we successfully replicated the original study, most importantly the modulation of delta phase consistency
615 by endogenous expectations. Our additional analyses support the interpretation as an oscillatory effect, rather than a
616 transient evoked response. Importantly, this work shows that the phase of delta oscillations is under endogenous control,
617 and hence qualifies as a possible mechanism for the neural implementation of (rhythmic) temporal predictions.

Power spectra, ERP muted: task (Cz)



Supplementary Figure 1: **Power Spectra computed of the task data after muting target-evoked responses**, all at electrode Cz. Left: Full power spectrum. Middle: Fractal power spectrum, computed using the irregular resampling technique. Right: Oscillatory spectrum, computed as the difference between the full and fractal spectra. Thick lines depict participant average, thin lines single participants' spectra. The blue shade in the right panel depicts the 98% confidence interval. The green dotted vertical line indicates the stimulation frequency (0.74 Hz). The topographies show the scalp distribution of power at 0.74 Hz.

619 References

- 620 Arnal, L. H., Doelling, K. B., and Poeppel, D. (2014). Delta–Beta Coupled Oscillations Underlie Temporal Prediction
621 Accuracy. *Cerebral Cortex*, page bhu103.
- 622 Arnal, L. H. and Giraud, A.-L. (2012). Cortical oscillations and sensory predictions. *Trends in Cognitive Sciences*,
623 16(7):390–398.
- 624 Barczak, A., O’Connell, M. N., McGinnis, T., Ross, D., Mowery, T., Falchier, A., and Lakatos, P. (2018). Top-down,
625 contextual entrainment of neuronal oscillations in the auditory thalamocortical circuit. *Proceedings of the National
626 Academy of Sciences*, 115(32):E7605–E7614.
- 627 Bates, D., Mächler, M., Bolker, B., and Walker, S. (2015). Fitting Linear Mixed-Effects Models Using lme4. *Journal of
628 Statistical Software*, 67(1):1–48.
- 629 Bauer, A.-K. R., Jaeger, M., Thorne, J. D., Bendixen, A., and Debener, S. (2015). The auditory dynamic attending
630 theory revisited: A closer look at the pitch comparison task. *Brain Research*, 1626:198–210.
- 631 Berens, P. (2009). CircStat: a MATLAB toolbox for circular statistics. *J Stat Softw*, 31(10):1–21.
- 632 Besle, J., Schevon, C. A., Mehta, A. D., Lakatos, P., Goodman, R. R., McKhann, G. M., Emerson, R. G., and Schroeder,
633 C. E. (2011). Tuning of the Human Neocortex to the Temporal Dynamics of Attended Events. *The Journal of
634 Neuroscience*, 31(9):3176–3185.
- 635 Bower, F. L., Fahrenfort, J. J., Millard, S. K., and Slagter, H. A. (2020). A silent disco: Persistent entrainment of
636 low-frequency neural oscillations underlies beat-based, but not memory-based temporal expectations. *bioRxiv*.
- 637 Brainard, D. H. (1997). The Psychophysics Toolbox. *Spatial Vision*, 10(4):433–436.
- 638 Breska, A. and Deouell, L. Y. (2017). Neural mechanisms of rhythm-based temporal prediction: Delta phase-locking
639 reflects temporal predictability but not rhythmic entrainment. *PLoS biology*, 15(2):e2001665.
- 640 Brunia, C. H. (2003). Cnv and spn: Indices of anticipatory behavior. In *The Bereitschaftspotential*, pages 207–227.
641 Springer.
- 642 Bruns, A. (2004). Fourier-, hilbert- and wavelet-based signal analysis: are they really different approaches? *Journal of
643 neuroscience methods*, 137(2):321–332.
- 644 Buzsáki, G. and Draguhn, A. (2004). Neuronal Oscillations in Cortical Networks. *Science*, 304(5679):1926–1929.
- 645 Cannon, J. (2021). Expectancy-based rhythmic entrainment as continuous bayesian inference. *PLOS Computational
646 Biology*, 17(6):e1009025.

- 647 Chang, A., Bosnyak, D. J., and Trainor, L. J. (2019). Rhythmicity facilitates pitch discrimination: Differential roles of
648 low and high frequency neural oscillations. *NeuroImage*.
- 649 Chaumon, M., Bishop, D. V., and Busch, N. A. (2015). A practical guide to the selection of independent components of
650 the electroencephalogram for artifact correction. *Journal of neuroscience methods*, 250:47–63.
- 651 Chou, E. P. and Hsu, S.-M. (2018). Cosine similarity as a sample size-free measure to quantify phase clustering within
652 a single neurophysiological signal. *Journal of neuroscience methods*, 295:111–120.
- 653 Cohen, M. X. (2014). *Analyzing neural time series data: theory and practice*. MIT press.
- 654 Coull, J. T., Davranche, K., Nazarian, B., and Vidal, F. (2013). Functional anatomy of timing differs for production
655 versus prediction of time intervals. *Neuropsychologia*, 51(2):309–319.
- 656 Cravo, A. M., Rohenkohl, G., Wyart, V., and Nobre, A. C. (2011). Endogenous modulation of low frequency oscillations
657 by temporal expectations. *Journal of Neurophysiology*, 106(6):2964–2972.
- 658 Cravo, A. M., Rohenkohl, G., Wyart, V., and Nobre, A. C. (2013). Temporal Expectation Enhances Contrast Sensitivity
659 by Phase Entrainment of Low-Frequency Oscillations in Visual Cortex. *The Journal of Neuroscience*, 33(9):4002–
660 4010.
- 661 Daume, J., Wang, P., Maye, A., Zhang, D., and Engel, A. K. (2021). Non-rhythmic temporal prediction involves phase
662 resets of low-frequency delta oscillations. *Neuroimage*, 224:117376.
- 663 Dercksen, T. T., Widmann, A., Schröger, E., and Wetzels, N. (2020). Omission related brain responses reflect specific
664 and unspecific action-effect couplings. *NeuroImage*, 215:116840.
- 665 Ding, N., Patel, A. D., Chen, L., Butler, H., Luo, C., and Poeppel, D. (2017). Temporal modulations in speech and
666 music. *Neuroscience & Biobehavioral Reviews*, 81:181–187.
- 667 Doelling, K. B. and Assaneo, M. F. (2021). Neural oscillations are a start toward understanding brain activity rather
668 than the end. *PLoS Biology*, 19(5):e3001234.
- 669 Edwards, E., Soltani, M., Kim, W., Dalal, S. S., Nagarajan, S. S., Berger, M. S., and Knight, R. T. (2009). Comparison
670 of time–frequency responses and the event-related potential to auditory speech stimuli in human cortex. *Journal of
671 neurophysiology*, 102(1):377–386.
- 672 Fisher, N. I. (1995). *Statistical analysis of circular data*. Cambridge University Press.
- 673 Giraud, A.-L. and Poeppel, D. (2012). Cortical oscillations and speech processing: emerging computational principles
674 and operations. *Nature Neuroscience*, 15(4):511–517.
- 675 Gross, J., Kujala, J., Hämäläinen, M., Timmermann, L., Schnitzler, A., and Salmelin, R. (2001). Dynamic imaging of
676 coherent sources: studying neural interactions in the human brain. *Proceedings of the National Academy of Sciences*,
677 98(2):694–699.
- 678 Halgren, M., Fabó, D., Ulbert, I., Madsen, J. R., Erőss, L., Doyle, W. K., Devinsky, O., Schomer, D., Cash, S. S., and
679 Halgren, E. (2018). Superficial slow rhythms integrate cortical processing in humans. *Scientific reports*, 8(1):1–12.
- 680 Helfrich, R. F., Fiebelkorn, I. C., Szczepanski, S. M., Lin, J. J., Parvizi, J., Knight, R. T., and Kastner, S. (2018). Neural
681 mechanisms of sustained attention are rhythmic. *Neuron*, 99(4):854–865.
- 682 Henry, M. J., Herrmann, B., and Obleser, J. (2014). Entrained neural oscillations in multiple frequency bands comodulate
683 behavior. *Proceedings of the National Academy of Sciences*, 111(41):14935–14940.
- 684 Henry, M. J., Herrmann, B., and Obleser, J. (2016). Neural Microstates Govern Perception of Auditory Input without
685 Rhythmic Structure. *Journal of Neuroscience*, 36(3):860–871.
- 686 Henry, M. J. and Obleser, J. (2012). Frequency modulation entrains slow neural oscillations and optimizes human
687 listening behavior. *Proceedings of the National Academy of Sciences*, 109(49):20095–20100.
- 688 Herbst, S. K., Fiedler, L., and Obleser, J. (2018). Tracking Temporal Hazard in the Human Electroencephalogram
689 Using a Forward Encoding Model. *eneuro*, 5(2):ENEURO.0017–18.2018.
- 690 Herbst, S. K. and Obleser, J. (2017). Implicit variations of temporal predictability: Shaping the neural oscillatory and
691 behavioural response. *Neuropsychologia*, 101:141–152.
- 692 Herbst, S. K. and Obleser, J. (2018). Implicit temporal predictability biases slow oscillatory phase in auditory cortex
693 and enhances pitch discrimination sensitivity. *bioRxiv*, page 410274.
- 694 Herbst, S. K. and Obleser, J. (2019). Implicit temporal predictability enhances pitch discrimination sensitivity and
695 biases the phase of delta oscillations in auditory cortex. *NeuroImage*, 203:116198.
- 696 Herrmann, B. and Henry, M. J. (2014). Low-Frequency Neural Oscillations Support Dynamic Attending in Temporal
697 Context. *Timing & Time Perception*, 2(1):62–86.

- 698 Herrmann, B., Henry, M. J., Haegens, S., and Obleser, J. (2016). Temporal expectations and neural amplitude
699 fluctuations in auditory cortex interactively influence perception. *NeuroImage*, 124, Part A:487–497.
- 700 Hincapié, A.-S., Kujala, J., Mattout, J., Pascarella, A., Daligault, S., Delpuech, C., Mery, D., Cosmelli, D., and Jerbi, K.
701 (2017). The impact of meg source reconstruction method on source-space connectivity estimation: a comparison
702 between minimum-norm solution and beamforming. *Neuroimage*, 156:29–42.
- 703 Jones, M. R. (1976). Time, our lost dimension: toward a new theory of perception, attention, and memory. *Psychological*
704 *Review*, 83(5):323–355.
- 705 Jones, M. R. (2018). *Time will tell: A theory of dynamic attending*. Oxford University Press.
- 706 Jones, M. R. and Boltz, M. (1989). Dynamic attending and responses to time. *Psychological review*, 96(3):459.
- 707 Jones, M. R., Moynihan, H., MacKenzie, N., and Puente, J. (2002). Temporal aspects of stimulus-driven attending in
708 dynamic arrays. *Psychological Science*, 13(4):313–319.
- 709 Keil, J., Pomper, U., and Senkowski, D. (2016). Distinct patterns of local oscillatory activity and functional connectivity
710 underlie intersensory attention and temporal prediction. *Cortex; a Journal Devoted to the Study of the Nervous*
711 *System and Behavior*, 74:277–288.
- 712 Kuznetsova, A., Brockhoff, P. B., and Christensen, R. H. B. (2016). *lmerTest: Tests in Linear Mixed Effects Models*. R
713 package version 2.0-30.
- 714 Kösem, A., Gramfort, A., and van Wassenhove, V. (2014). Encoding of event timing in the phase of neural oscillations.
715 *NeuroImage*, 92:274–284.
- 716 Lachaux, J.-P., Rodriguez, E., Martinerie, J., and Varela, F. J. (1999). Measuring phase synchrony in brain signals.
717 *Human brain mapping*, 8(4):194–208.
- 718 Lakatos, P., Gross, J., and Thut, G. (2019). A new unifying account of the roles of neuronal entrainment. *Current*
719 *Biology*, 29(18):R890–R905.
- 720 Lakatos, P., Karmos, G., Mehta, A. D., Ulbert, I., and Schroeder, C. E. (2008). Entrainment of Neuronal Oscillations as
721 a Mechanism of Attentional Selection. *Science*, 320(5872):110–113.
- 722 Lakatos, P., Musacchia, G., O’Connel, M. N., Falchier, A. Y., Javitt, D. C., and Schroeder, C. E. (2013). The
723 Spectrotemporal Filter Mechanism of Auditory Selective Attention. *Neuron*, 77(4):750–761.
- 724 Lakatos, P., Shah, A. S., Knuth, K. H., Ulbert, I., Karmos, G., and Schroeder, C. E. (2005). An oscillatory hierarchy
725 controlling neuronal excitability and stimulus processing in the auditory cortex. *Journal of neurophysiology*,
726 94(3):1904–1911.
- 727 Lange, K. (2013). The ups and downs of temporal orienting: a review of auditory temporal orienting studies and a
728 model associating the heterogeneous findings on the auditory N1 with opposite effects of attention and prediction.
729 *Frontiers in Human Neuroscience*, 7:263.
- 730 Large, E. W. and Jones, M. R. (1999). The dynamics of attending: How people track time-varying events. *Psychological*
731 *Review*, 106(1):119–159.
- 732 Lawrance, E. L. A., Harper, N. S., Cooke, J. E., and Schnupp, J. W. H. (2014). Temporal predictability enhances
733 auditory detection. *The Journal of the Acoustical Society of America*, 135(6):EL357–EL363.
- 734 Makeig, S., Westerfield, M., Jung, T.-P., Enghoff, S., Townsend, J., Courchesne, E., and Sejnowski, T. J. (2002).
735 Dynamic brain sources of visual evoked responses. *Science*, 295(5555):690–694.
- 736 Maris, E. and Oostenveld, R. (2007). Nonparametric statistical testing of EEG-and MEG-data. *Journal of neuroscience*
737 *methods*, 164(1):177–190.
- 738 MATLAB (2019). *version R2019a*. The MathWorks Inc., Natick, Massachusetts.
- 739 Mento, G. (2013). The passive CNV: carving out the contribution of task-related processes to expectancy. *Frontiers in*
740 *Human Neuroscience*, 7.
- 741 Morey, R. D. and Rouder, J. N. (2018). *BayesFactor: Computation of Bayes Factors for Common Designs*. R package
742 version 0.9.12-4.2.
- 743 Morillon, B., Arnal, L. H., Schroeder, C. E., and Keitel, A. (2019). Prominence of delta oscillatory rhythms in the
744 motor cortex and their relevance for auditory and speech perception. *Neuroscience & Biobehavioral Reviews*.
- 745 Morillon, B. and Baillet, S. (2017). Motor origin of temporal predictions in auditory attention. *Proceedings of the*
746 *National Academy of Sciences*, 114(42):E8913–E8921.
- 747 Morillon, B., Schroeder, C. E., Wyart, V., and Arnal, L. H. (2016). Temporal Prediction in lieu of Periodic Stimulation.
748 *The Journal of Neuroscience: The Official Journal of the Society for Neuroscience*, 36(8):2342–2347.

749 Neymotin, S. A., Tal, I., Barczak, A., O’Connell, M. N., McGinnis, T., Markowitz, N., Espinal, E., Griffith, E., Anwar,
750 H., Dura-Bernal, S., et al. (2021). Taxonomy of neural oscillation events in primate auditory cortex. *bioRxiv*, pages
751 2020–04.

752 Niemi, P. and Näätänen, R. (1981). Foreperiod and simple reaction time. *Psychological Bulletin*, 89(1):133–162.

753 Nozaradan, S., Peretz, I., Missal, M., and Mouraux, A. (2011). Tagging the Neuronal Entrainment to Beat and Meter.
754 *Journal of Neuroscience*, 31(28):10234–10240.

755 Obleser, J., Henry, M. J., and Lakatos, P. (2017). What do we talk about when we talk about rhythm? *PLOS Biology*,
756 15(9):e2002794.

757 Obleser, J. and Kayser, C. (2019). Neural entrainment and attentional selection in the listening brain. *Trends in cognitive
758 sciences*.

759 Oostenveld, R., Fries, P., Maris, E., and Schoffelen, J.-M. (2011). Fieldtrip: open source software for advanced analysis
760 of meg, eeg, and invasive electrophysiological data. *Computational intelligence and neuroscience*, 2011.

761 Oostenveld, R., Stegeman, D. F., Praamstra, P., and van Oosterom, A. (2003). Brain symmetry and topographic analysis
762 of lateralized event-related potentials. *Clinical neurophysiology*, 114(7):1194–1202.

763 Pelli, D. G. (1997). The VideoToolbox software for visual psychophysics: Transforming numbers into movies. *Spatial
764 vision*, 10(4):437–442.

765 Pernet, C. R., Wilcox, R. R., and Rousselet, G. A. (2013). Robust correlation analyses: false positive and power
766 validation using a new open source matlab toolbox. *Frontiers in psychology*, 3:606.

767 Popov, T., Oostenveld, R., and Schoffelen, J. M. (2018). Fieldtrip made easy: an analysis protocol for group analysis of
768 the auditory steady state brain response in time, frequency, and space. *Frontiers in neuroscience*, 12:711.

769 Praamstra, P., Kourtis, D., Kwok, H. F., and Oostenveld, R. (2006). Neurophysiology of Implicit Timing in Serial
770 Choice Reaction-Time Performance. *The Journal of Neuroscience*, 26(20):5448–5455.

771 Rimmele, J., Jolsvai, H., and Sussman, E. (2010). Auditory Target Detection Is Affected by Implicit Temporal and
772 Spatial Expectations. *Journal of Cognitive Neuroscience*, 23(5):1136–1147.

773 Rimmele, J. M., Morillon, B., Poeppel, D., and Arnal, L. H. (2018). The proactive and flexible sense of timing.

774 Rouder, J. N. (2014). Optional stopping: no problem for Bayesians. *Psychonomic Bulletin & Review*, 21(2):301–308.

775 Ruchkin, D. S., Sutton, S., Kietzman, M. L., and Silver, K. (1980). Slow wave and p300 in signal detection.
776 *Electroencephalography and Clinical Neurophysiology*, 50(1-2):35–47.

777 Saberi, K. and Hickok, G. (2021). Forward entrainment: Evidence, controversies, constraints, and mechanisms. *bioRxiv*.

778 Saleh, M., Reimer, J., Penn, R., Ojakangas, C. L., and Hatsopoulos, N. G. (2010). Fast and Slow Oscillations in Human
779 Primary Motor Cortex Predict Oncoming Behaviorally Relevant Cues. *Neuron*, 65(4):461–471.

780 SanMiguel, I., Saupé, K., and Schröger, E. (2013). I know what is missing here: electrophysiological prediction error
781 signals elicited by omissions of predicted” what” but not” when”. *Frontiers in human neuroscience*, 7:407.

782 Schmidt-Kassow, M., Schubotz, R. I., and Kotz, S. A. (2009). Attention and entrainment: P3b varies as a function of
783 temporal predictability. *Neuroreport*, 20(1):31–36.

784 Schroeder, C. E. and Lakatos, P. (2009). Low-frequency neuronal oscillations as instruments of sensory selection.
785 *Trends in Neurosciences*, 32(1):9–18.

786 Schröger, E., Marzecová, A., and SanMiguel, I. (2015). Attention and prediction in human audition: a lesson from
787 cognitive psychophysiology. *The European Journal of Neuroscience*, 41(5):641–664.

788 Schürmann, M., Başar-Eroglu, C., Kolev, V., and Başar, E. (2001). Delta responses and cognitive processing: single-trial
789 evaluations of human visual p300. *International Journal of Psychophysiology*, 39(2-3):229–239.

790 Stefanics, G., Hangya, B., Hernádi, I., Winkler, I., Lakatos, P., and Ulbert, I. (2010). Phase entrainment of human delta
791 oscillations can mediate the effects of expectation on reaction speed. *The Journal of neuroscience*, 30(41):13578–
792 13585.

793 Tallon-Baudry, C., Bertrand, O., Delpuech, C., and Pernier, J. (1996). Stimulus specificity of phase-locked and
794 non-phase-locked 40 hz visual responses in human. *Journal of Neuroscience*, 16(13):4240–4249.

795 Tzourio-Mazoyer, N., Landeau, B., Papathanassiou, D., Crivello, F., Etard, O., Delcroix, N., Mazoyer, B., and Joliot, M.
796 (2002). Automated anatomical labeling of activations in SPM using a macroscopic anatomical parcellation of the
797 MNI MRI single-subject brain. *Neuroimage*, 15(1):273–289.

798 van den Brink, R. L., Wynn, S. C., and Nieuwenhuis, S. (2014). Post-error slowing as a consequence of disturbed
799 low-frequency oscillatory phase entrainment. *Journal of Neuroscience*, 34(33):11096–11105.

- 800 van Diepen, R. M. and Mazaheri, A. (2018). The caveats of observing inter-trial phase-coherence in cognitive
801 neuroscience. *Scientific reports*, 8(1):1–9.
- 802 Walter, W. G., Cooper, R., Aldridge, V. J., McCallum, W. C., and Winter, A. L. (1964). Contingent Negative Variation :
803 An Electric Sign of Sensori-Motor Association and Expectancy in the Human Brain. *Nature*, 203:380–384.
- 804 Wen, H. and Liu, Z. (2016). Separating fractal and oscillatory components in the power spectrum of neurophysiological
805 signal. *Brain topography*, 29(1):13–26.
- 806 Widmann, A., Schröger, E., and Maess, B. (2015). Digital filter design for electrophysiological data – a practical
807 approach. *Journal of Neuroscience Methods*, 250:34–46.
- 808 Wilsch, A., Henry, M. J., Herrmann, B., Maess, B., and Obleser, J. (2015). Slow-delta phase concentration marks
809 improved temporal expectations based on the passage of time. *Psychophysiology*, 52(7):910–918.
- 810 Winkler, I., Debener, S., Müller, K.-R., and Tangermann, M. (2015). On the influence of high-pass filtering on ica-based
811 artifact reduction in eeg-erp. In *2015 37th Annual International Conference of the IEEE Engineering in Medicine
812 and Biology Society (EMBC)*, pages 4101–4105. IEEE.
- 813 Woodrow, H. (1914). *The Measurement of Attention (1914)*, volume The Psychological Monographs 17(5). Google-
814 Books-ID: Jr5nRQAACAAJ.
- 815 Wright, B. A. and Fitzgerald, M. B. (2004). The time course of attention in a simple auditory detection task. *Perception
816 & Psychophysics*, 66(3):508–516.
- 817 Zalta, A., Petkoski, S., and Morillon, B. (2020). Natural rhythms of periodic temporal attention. *Nature communications*,
818 11(1):1–12.
- 819 Zoefel, B. and Heil, P. (2013). Detection of near-threshold sounds is independent of eeg phase in common frequency
820 bands. *Frontiers in psychology*, 4:262.
- 821 Zoefel, B., ten Oever, S., and Sack, A. T. (2018). The Involvement of Endogenous Neural Oscillations in the Processing
822 of Rhythmic Input: More Than a Regular Repetition of Evoked Neural Responses. *Frontiers in Neuroscience*, 12.